TECHNISCHE UNIVERSITÄT MÜNCHEN
TUM School of Life Sciences

Mechanistic understanding of coupled carbon-nitrogen-phosphorus cycling for climate-smart management in temperate soils

Kaiyu Lei

Vollständiger Abdruck der von der TUM School of Life Sciences
der Technischen Universität München zur Erlangung eines
Doktors der Naturwissenschaften (Dr. rer. nat.)
genehmigten Dissertation.

Vorsitz:		Prof. Dr. Martin Wiesmeier
Prüfende der Dissertation:	1.	Prof. Dr. Dr. h.c. Ingrid Kögel-Knabner
	2.	Prof. Dr. Roland Bol

Die Dissertation wurde am 05.06.2025 bei der Technischen Universität München eingereicht und durch die TUM School of Life Sciences am 31.07.2025 angenommen.

„*Per Aspera Ad Astra*“

循此苦旅，以达星辰

I Summary

Facing escalating climate change and phosphorus (P) fertilizer scarcity, temperate soils must concurrently sustain agricultural productivity by ensuring phosphorus availability and function as carbon (C) sinks. However, intensive cropland use typically reduces soil organic carbon (SOC), negatively affecting the soil agricultural and ecological functions. Cropland soils commonly depend on P derived from inorganic phosphorus (IP) pools, which, despite high immediate availability, are prone to loss via leaching and soil erosion. Organic phosphorus (OP), derived from organic matter (OM) decomposition, emerges as a sustainable alternative. Nonetheless, OP utilization remains limited due to an insufficient mechanistic understanding of its stabilization and availability under contrasting land uses. Knowledge gaps persist regarding coupled carbon-nitrogen-phosphorus (C-N-P) cycling, impeding climate-smart management application in temperate soils.

To address these challenges, this work aims to deepen the mechanistic understanding of the stabilization and availability pathways of P under contrast land uses and provide possible strategies to enhance carbon sequestration and nutrient retention in temperate cropland soils. This work integrated particle-size fractionation, stoichiometric analysis, and nanoscale secondary ion mass spectrometry (NanoSIMS) measurements to reveal detailed insights into C, N, and P stocks and their vertical distribution patterns across two contrasting land uses (grassland vs. cropland) and distinct soil development processes (hillslope vs. flood plain). By bridging well-documented OC cycling mechanisms with P cycling, this work sought to identify specific pathways governing P retention and availability with the additional direct organo-mineral observations via NanoSIMS, thereby delineating the potential use of OP for sustainable P utilization. To further counteract the degraded C stocks of cropland soils, this work evaluated enhanced rock weathering (ERW) strategy as an alternative to traditional liming, aiming to simultaneously correct soil acidity and guarantee long-term carbon sequestration.

This work demonstrated that land use practices and soil development processes shape elements (C, N and P) cycling significantly and distinctly. Temperate grassland soils exhibited higher OC and N stocks compared to cropland soils (Study I), whereas total P stocks remained the same, with grassland soils retaining a high P availability comparable to cropland soils (Study II). Specifically, grassland soils exhibited higher OC storage throughout the soil profile due to greater OM inputs and well-preserved subsoil structures. In contrast, cropland soils showed a lower OC stock, which resulted from continuous soil structure degradation and less OM inputs via clear harvest. Total P stocks were marginally affected by land uses due to their primary originating from parent material as IP. Instead, the partitioning of IP and OP varied significantly between the two land uses due to different OM inputs and preservation in the

topsoils. Grassland topsoils showed the dominance of OP, whereas IP dominated cropland topsoils, though overall P availability remained similar between the two land uses (Study I; Study II).

Both OC and OP were enriched and concentrated in the fine soil (<20 μm, Study I). Further stoichiometric analysis combined with NanoSIMS measurements of these fine soils revealed two P retention pathways coupled distinctly to OC and organic N (Study I; Study II). In these temperate grassland soils, large amounts of C, N and P were immobilized within OM, including those assimilated within microbial biomass/necromass, with a few IP-mineral complexes observed on microaggregate surfaces. The immobilized OP was subsequently available through microbial mineralization processes facilitated by high OC content. In contrast, these temperate cropland soils primarily retain P as IP-mineral complexes, particularly IP-phyllosilicate complexes. These IP-mineral complexes exhibited weaker sorption strength, making P readily accessible via desorption. Thus, grassland management with abundant OP pools could also ensure high P availability. The effectiveness was attributed largely to the abundance of clay-sized phyllosilicates strongly associated with OM, which concurrently serve as key sinks for OC, organic N and OP. Therefore, this study suggests that sustaining high levels of OC and N are critical to achieving sustainable use of OP pools (Study II).

To reverse the degraded structure and OC storage of long-term cropland use soils, this work mechanistically explored fine silicate rock (fresh/weathered basalt powder) amendments as an effective strategy for long-term carbon sequestration (Study III). These amendments not only corrected soil acidity and provided essential macronutrients to support agricultural productivity but also facilitated sustained inorganic carbon (IC) sequestration. Although fresh basalt amendments initially caused SOC losses due to rapid H^+ neutralization, they could be offset during subsequent weathering due to better OC retention observed in weathered basalt amendments (Study III). Specifically, weathered basalt, depleted in reactive olivine minerals, demonstrated limited pH elevation and enhanced the retention of both native and new OM derived from biomass inputs due to increased specific surface areas and exchangeable calcium (Ca) contents. Moreover, weathered basalt continued to accumulate IC as fresh basalt through slow mineral dissolution, further promoting the overall carbon sequestration capacity. Continuous inputs of new OM into cropland soils generated additional acidity, potentially competing with mineral dissolution processes critical to ERW effectiveness. Study III thus indicated that in such slightly acidic cropland soils, the continuous new OM inputs might constrain IC sequestration by reducing dissolved IC accumulation. Consequently, ERW in these contexts primarily enhances SOC stabilization rather than substantial IC storage. Basalt amendments at both weathering stages consistently supplied P, suggesting potential additional benefits as a slow-released P fertilizer.

This work reveals contrasting C, N, and P cycling patterns in temperate cropland and grassland soils. Cropland soils exhibit relatively weaker coupled N-P correlations and reduced OP stocks due to less OM inputs and high reliance on IP-phyllosilicate complexes, while grassland soils sustain stronger coupled N-P cycling and higher OC and OP stocks through microbial-driven organo-mineral interactions. Thereby, despite their comparable P availability, grassland soils primarily retain OP pools within microbial biomass and OM, maintaining high OC and N levels to sustain microbial turnover, whereas cropland soils depend on weaker IP desorption. To counter OC degradation in cropland soils, ERW strategy with basalt amendments emerges as a solution, which corrects soil acidity, supplies additional nutrients, and promotes long-term carbon sequestration via IC accumulation and enhanced OC retention for new OM, albeit with trade-offs (e.g., initial OC loss with fresh basalt).

Therefore, integrating these mechanistic insights from contrasting temperate ecosystems (grassland vs. cropland) and emerging ERW strategy, this work highlights several climate-smart management options for temperate soils. Maintaining minimal disturbance and regular organic inputs in extensively managed grasslands preserves soil structure, enhancing OC, N, and P stocks critical for carbon sequestration and sustainable productivity. For intensively managed croplands facing OM depletion and phosphorus losses, combining organic amendments with ERW provides an effective solution, improving soil structure, acidity correction, and nutrient retention, thereby promoting long-term soil sustainability and agricultural productivity.

II Zusammenfassung

Angesichts des zunehmenden Klimawandels und der Knappheit an Phosphor (P) - Düngemitteln müssen gemäßigte Böden gleichzeitig verschiedene Funktionen erfüllen. Einerseits müssen sie die landwirtschaftliche Produktivität durch ausreichende Phosphorverfügbarkeit aufrechterhalten und andererseitsd als Kohlenstoff-Senken fungieren. Die intensive Nutzung von Ackerland führt jedoch typischerweise zu einem Rückgang des organischen Bodenkohlenstoffs (SOC), was die landwirtschaftlichen und ökologischen Funktionen der Böden negativ beeinflusst. Ackerböden sind häufig auf anorganische Phosphor (IP) angewiesen, die zwar sofort verfügbar sind, jedoch leicht durch Auswaschung und Erosion verloren gehen. Organischer Phosphor (OP), der aus dem Abbau organischer Substanz (OM) stammt, stellt eine nachhaltige Alternative dar. Die Nutzung von OP ist jedoch begrenzt, da unser Verständnis seiner Stabilisierungs- und Verfügbarkeitsmechanismen Lücken aufweist. Diese Wissenslücken, die häufig die gekoppelten Kohlenstoff-Stickstoff-Phosphor (C-N-P) Kreisläufe betreffen, verhindern die Umsetzung nachhaltiger Bewirtschaftungsstrategien der Böden.

Zur Bewältigung dieser Herausforderungen zielt diese Arbeit darauf ab, das mechanistische Verständnis der Stabilisierung und Verfügbarkeit von Phosphor unter unterschiedlichen Landnutzungen zu vertiefen und Strategien zur Steigerung der Kohlenstoffspeicherung und Nährstoffretention in gemäßigten Ackerböden bereitzustellen. Dazu wurden Partikelgrößenfraktionierung, stöchiometrische Analysen sowie nanoskalige Sekundärionen-Massenspektrometrie (NanoSIMS)-Messungen kombiniert, um detaillierte Einblicke in die C-, N- und P-Vorräte sowie deren vertikale Verteilungsmuster unter zwei kontrastierenden Landnutzungen (Grünland vs. Ackerland) und unterschiedlichen Bodenprozessen (Hanglage vs. Auenebene) zu gewinnen. Durch die Verknüpfung gut erforschter Prozesse des organischen Kohlenstoffkreislaufs (OC) mit dem Phosphorkreislauf verbunden wurden, sollten spezifische Pfade der P-Retention und -Verfügbarkeit durch direkte organo-mineralische Beobachtungen mittels NanoSIMS identifiziert werden, um so das Potenzial von OP für eine nachhaltige P-Nutzung zu skizzieren. Zur weiteren Verbesserung der reduzierten C-Vorräte in Ackerböden wurde zudem die Strategie der „Enhanced Rock Weathering“ (ERW) als Alternative zur herkömmlichen Kalkung evaluiert, um zugleich Bodenversauerung zu neutralisierten und langfristige Kohlenstoffspeicherung zu gewährleisten.

Diese Arbeit zeigte deutlich, dass Landnutzung und Bodenprozesse die Elementkreisläufe (C, N und P) signifikant und spezifisch beeinflussen. Grünlandböden wiesen höhere OC- und N-Vorräte als Ackerböden auf (Studie I), während die Gesamt-P-Vorräte ähnlich blieben und Grünlandböden eine vergleichbar hohe P-Verfügbarkeit wie Ackerböden aufwiesen (Studie II). Höhere OC-Vorräte in Grünlandböden ergaben sich aus gesteigerten OM Einträgen und

intakten Unterbodenstrukturen, während in Ackerböden reduzierte OC-Vorräte auf strukturelle Degradation und geringere OM Einträge durch regelmäßige Ernten zurückzuführen waren. Die Gesamt-P-Vorräte waren kaum landnutzungsabhängig. Allerdings unterschieden sich IP- und OP-Anteile zwischen den Landnutzungen aufgrund unterschiedlicher OM Einträge und deren Erhaltung in Oberböden. Während OP in Grünlandböden dominierte, herrschte IP in Ackerböden vor, wobei die Gesamtverfügbarkeit von P vergleichbar blieb (Studie I; Studie II).

OC und OP konzentrierten sich insbesondere im Feinbodenfraktionen (<20 µm, Studie I). Weitere stöchiometrische Analysen und NanoSIMS-Messungen dieser Feinbodenfraktion zeigten zwei unterschiedliche P-Retentionspfade, gekoppelt an OC und organischen N (Studie I; Studie II). In Grünlandböden erfolgte die Immobilisierung großer Mengen von C, N und P in OM einschließlich mikrobieller Biomasse/Nekromasse, wobei wenige IP-Mineralkomplexe auf Mikroaggregatoberflächen beobachtet wurden. Der immobilisierte OP war über mikrobielle Mineralisierungsprozesse durch den hohen OC-Gehalt verfügbar. Im Gegensatz dazu speicherten Ackerböden P hauptsächlich als IP-Mineralkomplexe, insbesondere IP-Phyllosilikat-Komplexe. Diese Komplexe zeigten eine schwächere Sorptionsstärke und machten P leicht durch Desorption verfügbar. Grünlandböden mit reichlich OP konnten daher eine ebenso hohe P-Verfügbarkeit gewährleisten. Die Effektivität wurde maßgeblich auf den hohen Anteil tonreicher Phyllosilikate zurückgeführt, die eng an OM gebunden sind und zugleich wichtige Senken für OC, organischen N und OP darstellen. Diese Studie hebt hervor, dass hohe OC- und N-Gehalte essenziell sind, um eine nachhaltige Nutzung der OP-Pools sicherzustellen (Studie II).

Zur Behebung der strukturellen Degradation und reduzierter OC-Vorräte in Ackerböden wurde die Zugabe von silikatischem Gestein (frisches/verwittertes Basaltpulver) untersucht (Studie III). Diese Zugaben korrigierten nicht nur die Bodensäure, sondern lieferten essenzielle Makronährstoffe und förderten eine langfristige Speicherung von anorganischem Kohlenstoff (IC). Obwohl frischer Basalt zunächst OC-Verluste verursachte, konnten diese bei weiterer Verwitterung kompensiert werden wobei in verwittertem Basalt eine bessere OC-Retention beobachtet wurde. Verwitterter Basalt erhöhte aufgrund höherer spezifischer Oberflächen und austauschbarer Calcium-Gehalte effektiv die Retention sowohl nativer als auch neuer OM. Basaltzugaben lieferten kontinuierlich P und zeigten somit zusätzliches Potenzial als langsam freisetzender P-Dünger.

Diese Arbeit zeigt gegensätzliche Muster des C-, N- und P-Kreisläufe in Acker- und Grünlandböden der gemäßigten Zonen. Ackerböden weisen schwächere gekoppelte N-P-Korrelationen und geringere OP-Vorräte auf, was auf geringere OM-Einträge und die Abhängigkeit von IP-Phyllosilikat-Komplexen zurückzuführen ist, während Grünlandböden einen stärkeren gekoppelten N-P-Kreislauf und höhere OC- und OP-Vorräte durch mikrobiell

angetriebene organisch-mineralische Interaktionen aufweisen. Trotz ihrer vergleichbaren P-Verfügbarkeit setzen Grünlandböden vorrangig auf die OP-Retention in der mikrobiellen Biomasse und im OM und erhalten hohe OC- und N-Gehalte, um den mikrobiellen Umsatz aufrechtzuerhalten, während Ackerböden auf eine schwächere IP-Desorption angewiesen sind. Um dem OC-Abbau in Ackerböden entgegenzuwirken, erweist sich die ERW-Strategie mit Basaltzusätzen als Lösungen, die den Bodenversauerung neutralisiert, zusätzliche Nährstoffe liefert und die langfristige Kohlenstoffbindung durch IC-Akkumulation und verbesserte OC-Retention für neue OM fördert, wenn auch mit Abstrichen (z. B. anfänglicher OC-Verlust mit frischem Basalt).

Durch die Integration mechanistischer Erkenntnisse aus kontrastierenden Ökosystemen der gemäßigten Breiten (Grünland und Ackerland) und einer neuen ERW-Strategie werden in dieser Arbeit klimafreundliche Bewirtschaftungsoptionen für Böden der gemäßigten Breiten aufgezeigt. Die Beibehaltung minimaler Störungen und regelmäßiger OM Einträge in extensiv bewirtschaftetem Grünland bewahrt die Bodenstruktur und erhöht die OC-, N- und P-Vorräte, die für die Kohlenstoffspeicherung und nachhaltige Produktivität entscheidend sind. Für intensiv bewirtschaftete Ackerland, die mit einer Verarmung an OM und Phosphorverlusten konfrontiert sind, bietet die Kombination von organischer Düngemittel mit ERW eine wirksame Lösung, die die Bodenstruktur verbessert, den Säuregehalt neutralisiert und Nährstoffe zurückhält und so die langfristige Nachhaltigkeit des Bodens und die landwirtschaftliche Produktivität fördert.

III List of studies

This dissertation is based on the following first-authored studies. Published studies are attached as appendices A-B. Study II has not yet been published, which is treated separately as appendix C.

Study I	
Title	Distinct impact of land use and soil development processes on coupled biogeochemical cycling of C, N and P in a temperate hillslope-flood plain system
Author	**Kaiyu Lei***, Franziska B. Bucka, Christopher Just, Sigrid van Grinsven, Sebastian Floßmann, Michael Dannenmann, Jörg Völkel, Ingrid Kögel-Knabner
Publication	Biogeochemistry 168, 21 (2025). DOI: 10.1007/s10533-025-01213-y
Objectives	- Understand carbon (C), nitrogen (N) and phosphorus (P) stocks and their stoichiometric correlation in soils under contrast land uses and soil development processes - Investigate distribution and enrichment of C and P in different soil fractions - Deepen the understanding of organic phosphorus (OP) cycling and turnover in soils under contrast land uses
Summary	This study demonstrates that land use and soil development processes distinctly shape soil C, N, and P stocks. On hillslopes with comparable soil development, grassland soils show higher organic carbon (OC) and total nitrogen (TN) accumulation through higher organic matter inputs and better-preserved soil structure, whereas cropland soils show the opposite due to lower inputs and soil degradation. The OP content and OP/inorganic phosphorus (IP) partitioning are sensitive to the land use. A higher IP content in cropland topsoil compensates for lower subsoil OP content, resulting in similar total phosphorus (TP) stocks between land uses. Conversely, flood plain soils, influenced by sedimentation and hydrology, show substantial subsoil enrichment of OC, TN, and IP, with land use impacts mostly limited to topsoils. Stoichiometric analyses reveal greater OC and OP enrichment in fine fractions. The OC:OP ratio suggests two distinct OP retention pathways: microbial biomass assimilation (biotic pathway) and direct mineral association (abiotic pathway). By combining stoichiometric assessments with physical fractionation, this study highlights mechanisms for sustainable OP

	management and illustrates how maintaining OC and N levels may support P availability in soils.
Contribution	Conception, material acquisition, soil analysis and data analysis, draft and revision of manuscript with input from co-authors

Study II	
Title	Phyllosilicates determine the retention and availability of P in temperate soils
Author	**Kaiyu Lei***, Franziska B. Bucka, Carmen Hoeschen, Yahan Hu, Ingrid Kögel-Knabner
Publication	Unpublished
Objectives	- Develop a method to distinguish inorganic (IP) and organic phosphorus (OP) on microaggregates based on NanoSIMS measurements - Investigate their respective spatial distribution on microaggregate surfaces - Delineate retention pathways of phosphorus (P) on microaggregate surfaces based on direct observations
Summary	This study introduces a novel method for directly visualizing and differentiating IP and OP on soil microaggregate surfaces, highlighting the significant role of phyllosilicates and their associated organic matter (OM) in P retention and availability. Our findings confirm the simultaneous presence of two distinct P retention pathways: soils with abundant OM-free mineral surfaces predominantly retain IP through IP-phyllosilicate complexes, while OM-rich soils primarily immobilize OP in OM associated with phyllosilicates. This perspective demonstrates that the sustainable utilization of OP as an alternative to IP fertilizers requires maintaining adequate levels of soil organic carbon (OC) and nitrogen (N) and suggests updating existing models of soil P dynamics to better incorporate phyllosilicate minerals and OM interactions in temperate soils.
Contribution	Conception, assistant NanoSIMS measurements, image and data analysis, draft and revision of manuscript with input from co-authors

Study III

Title:	Balance organic and inorganic carbon in enhanced rock weathering: Implication for carbon sequestration
Author:	**Kaiyu Lei***, Franziska B. Bucka, Pedro P. C. Teixeira, Franz Buegger, Christopher Just, Ingrid Kögel-Knabner
Publication	Global Change Biology 31, 4 (2025). DOI: 10.1111/gcb.70186
Objectives	- Clarify the interaction between organic carbon (OC) and inorganic carbon (IC) associated with enhanced rock weathering (ERW) - Assess the long-term effectiveness of ERW on carbon sequestration - Understand new organic matter (OM) inputs on the effectiveness of carbon sequestration associated with ERW
Summary	This study reveals that the stage of basalt weathering plays a critical role in regulating soil carbon dynamics and fluxes in temperate cropland topsoils. Over a six-month incubation, both fresh and weathered basalt amendments enhanced soil inorganic carbon (SIC) accumulation. Fresh basalt, enriched in olivine, increases soil pH via rapid H^+ neutralization and increases bicarbonate alkalinity, promoting dissolved inorganic carbon (DIC) formation and subsequent SIC accrual. However, this also leads to soil organic carbon (SOC) losses. In contrast, weathered basalt, depleted in olivine, does not significantly alter soil pH, resulting in SOC losses similar to the control soils. Nevertheless, it continues to support SIC accumulation via slower reactions with less-reactive minerals and elevated Ca^{2+} release. Moreover, weathered basalt shows improved retention of both native and straw-derived new OC, likely due to its higher surface area and Ca-mediated stabilization. The presence of continuous OM inputs alters ERW outcomes. These residues acidify the soil through OM decomposition, competing with carbonic acid for mineral dissolution, thereby reducing DIC formation and SIC gains. Overall, the findings emphasize that for ERW to be effective as a climate mitigation strategy, SOC stabilization must be prioritized, especially in ecosystems with continuous OM inputs. In the long term, basalts, with their benefits for C retention (with weathering processes) and acidity correction, show strong potential as an alternative to lime in acidic agricultural soils.

Contribution	Conception, material acquisition, microcosms study setup and processing, soil analysis and data analysis, draft and revise manuscript with input from co-authors

IV Table of Content

Content

I Summary I
II Zusammenfassung IV
III List of studies VII
IV Table of Content XI
1 Introduction 1
1.1 Soil organic carbon, nitrogen, phosphorus stocks under different land uses and soil development processes in temperate zones 1
1.2 Soil organic matter physical fractionation and its implications 2
1.3 Element stoichiometry as a tool for understanding biogeochemical cycling 4
1.4 Stabilization processes of soil inorganic and organic phosphorus 5
1.5 Nano-scale secondary ion mass spectrometry (NanoSIMS) as a tool for organo-mineral interaction studies 9
1.6 Silicate mineral weathering as a potential strategy for nutrient supply and carbon sequestration under climate change 10
1.7 Objectives and approaches 14
2 Material and Methods 17
2.1 Study site and soil description 17
2.1.1 Study site description (Study I) 17
2.1.2 Soil description (Study I, II, III) 18
2.2 Incubation experiment setup and sampling (Study III) 19
2.3 Soil physicochemical analyses (Study I, II, III) 20
2.3.1 Soil pH (Study I, II, III) 20
2.3.2 Soil particle size distribution (Study I, III) 20
2.3.3 Specific surface area analysis (Study III) 21
2.3.4 Soil effective cation exchange capacity and exchangeable cations analysis (Study III) 21
2.3.5 Soil total element analysis (Study I, III) 21
2.3.6 TC, SOC, SIC, $\delta^{13}C$ and $\delta^{15}N$ analysis (Study I, II, III) 21
2.3.7 Organic phosphorus (OP), inorganic phosphorus (IP) and available phosphorus analysis (Study I, II) 22
2.3.8 Particle size fractionation (Study I, II, III) 22
2.3.9 Mineral characterization (Study II, III) 22
2.4 Microscale analyses (Study II) 22
2.4.1 Sample preparation and optical microscopy measurements 22
2.4.2 NanoSIMS measurements 23
2.5 Statistical analyses (Study I, II, III) 23
3 Results 25

3.1 Results summary of Study I & III 25
3.1.1 Bulk soil OC, TN, TP, OP, IP contents, and $\delta^{15}N$ signature (Study I) 25
3.1.2 Bulk soil OC, TN, TP, OP and IP stocks (Study I) 26
3.1.3 Molecular components of bulk soil derived from solid-state ^{13}C NMR spectroscopy (Study I) 26
3.1.4 The distribution and enrichment of OC and OP in the fine and coarse fractions (Study I) 27
3.1.5 OC:TN ratio to OC:OP ratio and their correlation with OC in bulk soils, fine and coarse soil fractions (Study I) 27
3.1.6 Soil C contents, $\delta^{13}C$ analysis and physicochemical properties after 6-months of incubation (Study III) 28
3.1.7 Random Forest model for explaining SOC and SIC contents (Study III) 28
3.1.8 The C balance and fluxes in the atmosphere-soil-effluent system (Study III) 29
3.2 Results summary of the unpublished Study II 29
4 Discussion 31
4.1 Distinct effect of land use and soil development processes on carbon, nitrogen and phosphorus cycling in the flood plain and hillslope in temperate zones 31
4.2 The two potential pathways for phosphorus retention and availability associated with organic carbon and nitrogen cycling 36
4.3 The role of phyllosilicates in maintaining carbon and phosphorus pools in temperate soils 41
4.4 Silicate rock powder amendment as a strategy for long-term carbon sequestration for cropland soils 44
4.5 Implications for targeting climate-smart management options in temperate soils 48
5 Reference 49
6 Acknowledgement 59
7 Appendix 61
A Study I 61
B Study III 62
C Study II 63
D Scientific contributions 64

1 Introduction

1.1 Soil organic carbon, nitrogen, phosphorus stocks under different land uses and soil development processes in temperate zones

Land use significantly influences carbon (C), nitrogen (N), and phosphorus (P) stocks in temperate zones, playing a crucial role in terrestrial ecosystem functions and sustainability. Among the various forms of terrestrial soil carbon, soil organic carbon (SOC) constitutes the most abundant form, significantly regulating carbon cycling and storage in temperate regions (Fu et al., 2010; Guo and Gifford, 2002; Poeplau et al., 2011; Sigua and Coleman, 2010; Wiesmeier et al., 2020; Wiesmeier et al., 2012; Wu and Tiessen, 2002). The state of Bavaria in Germany has a typical temperate landscape, predominantly comprising grasslands, croplands and forests distributed across hillslopes and flood plains within the Bavarian Forest (Wiesmeier et al., 2014). Grasslands generally store greater SOC stocks compared to croplands, evident in both topsoil (0-20/30 cm) and deeper subsoil horizons (>30 cm) (Mayer et al., 2019).

In contrast, cropland soil typically exhibits reduced SOC and N stocks, primarily due to soil erosion contributing to intensive agricultural practices such as ploughing and clear-harvest. These practices can degrade soil structure, accelerate the mineralization of soil organic matter (SOM) (Hamza and Anderson, 2005; Six et al., 1998), and limit the input of new organic matter (OM). These factors collectively lead to substantial declines in SOC stocks following the conversion from grassland to cropland, which is widely observed across temperate regions. However, soil type, a factor intrinsically linked to soil development processes, can also considerably influence SOC storage (Wiesmeier et al., 2014; Wiesmeier et al., 2012; Wiesmeier et al., 2015), yet only limited studies have considered this factor. Neglecting the impact of soil development processes when assessing land use effects can result in significant underestimation of SOC stocks, particularly in cultivated soils (Wiesmeier et al., 2015).

The influence of land use is generally considered more critical for topsoil organic carbon (OC) stocks than subsoils, with more studies realizing the large contribution of SOC stocks from subsoils (Rumpel and Kögel-Knabner, 2011), which can thereby be dependent on soil development processes. Due to limited air exchange and reduced water infiltration rates, subsoil OC stocks are primarily regulated by below-ground biomass and soil development processes, including pedogenic processes (Kögel-Knabner and Amelung, 2021), alluvial and colluvial processes (Mayer et al., 2019). Flood plain soils are particularly influenced by subsoil, as their subsoils experience periodic flooding and sedimentation, resulting in substantially higher SOC stocks across the entire soil profile compared to adjacent soils on the hillslope (Chaopricha and Marín-Spiotta, 2014; D'Elia et al., 2017; Hoffmann et al., 2013; Mayer et al.,

2018; Sutfin et al., 2016), with intensive cropland use on the slope leading to significant sedimentation in the flood plain (Doetterl et al., 2025). Therefore, accurate assessment and prediction of SOC stocks must incorporate both land use practices and inherent soil development processes.

In contrast to the extensively studied cycling of SOC and N, the impact of land use on total phosphorus (TP) storage remains debatable. Phosphorus storage depends heavily on multiple factors, including climatic conditions, vegetation types, fertilizer inputs and soil development processes. Given that rock-derived minerals represent a primary P source, parent materials significantly influence soil TP stocks, particularly in subsoil horizons where organic phosphorus (OP) inputs via SOM are comparatively limited. In temperate regions, inorganic phosphorus (IP) typically constitutes 30% to 70% of TP stocks, with subsoils contributing 25%-70% of the stocks (Gocke et al., 2021; Kautz et al., 2013; Stutter et al., 2015). A recent P inventory across Germany highlights substantial P reserves in subsoils, emphasizing their potential for sustainable agricultural utilization and their importance in offsetting topsoil P depletion resulting from intensive agriculture (Gocke et al., 2021). The substantial subsoil contribution to TP storage suggests that, in addition to land use, soil development processes can critically determine soil P stocks. Despite this fact, most P studies attribute variations in P stocks solely to land use practices, overlooking differences introduced by distinct soil development processes.

Furthermore, transitioning natural vegetation into croplands distinctly affects the partitioning between IP and OP stocks, although IP remains dominant (Alt et al., 2011; Hedley et al., 1982; Kopittke et al., 2017). The long-term cropland use in temperate zones can decrease P diversity, especially OP abundance and species, while grassland use can reverse the IP-dominant TP stocks to OP-dominant TP stocks, which suggests strong microbial-mediated processes (Stutter et al., 2015). Thus, partitioning can potentially shape P dynamics and availability in ecosystems due to the significant differences in stability and ecological accessibility between IP and OP fractions. A mechanistic understanding of their distribution and amounts in landscape scales as well as microscale is thereby critical for better phosphorus management in temperate soils.

1.2 Soil organic matter physical fractionation and its implications

To mechanistically evaluate OC and OP cycling under contrast land uses and soil development processes, it is crucial to consider not only the quantity but also the stability and turnover of these organic pools. This is particularly important in the context of changing climate, as these factors significantly influence the biogeochemical cycling of these elements.

Soil organic matter broadly includes both undecomposed and decomposed plant and animal residues, as well as their organic transformation by-products. One of the most essential and effective ways to understand the stability and turnover of SOM in mineral soils is soil fractionation. One of the methods is physical fractionation, of which particle-size fractionation and density fractionation are two of the most widely applied fractionation methods to distinguish OC fractions with distinct turnover times. Specifically, particle size fractionation is mostly used for distinguishing turnover between OC pools (Just et al., 2021; von Lützow et al., 2008), while density fractionation aims to isolate particulate organic matter (POM) from SOM that is associated with soil minerals or occluded in aggregates (Christensen et al., 1992; von Lützow et al., 2008). Both methods can sufficiently fractionate the SOM into POM and mineral-associated organic matter (MAOM) based on their respective criteria, which represent fractions with relatively short and long turnover times, respectively (Just et al., 2021; Schmidt et al., 2011). All particle size fractionation and some density fractionation protocols involve procedures that disperse soil aggregates, such as with water, with sodium metaphosphate (Tyner, 1940), with ultrasonication (Just et al., 2021; Kölbl et al., 2005), or with glass beads (Chenu and Plante, 2006), to free occluded POM fractions from soil aggregates.

The POM fraction primarily consists of less-decomposed, high-molecular-weight OM, commonly derived from above- and below-ground plant biomass and organic amendments such as manure or compost. It is mainly concentrated in particles with a density lower than 1.6-1.85 g/cm^3 or particle size larger than 20/50/63 µm (Christensen, 1996; Lavallee et al., 2020), whose threshold highly depending on soil texture (Just et al., 2021). In contrast, the MAOM fraction encompasses OC stabilized through associations with mineral surfaces via ligand exchange (inner-sphere complexation), electrostatic adsorption, hydrogen and cation bridging, as well as incorporation into microbial biomass/necromass. The microbial biomass/necromass can contribute up to 50% of MAOM-C (Angst et al., 2021; Kögel-Knabner, 2002; Wang et al., 2021), underscoring their critical role not only in stabilizing MAOM but also in promoting the decomposition of POM. Due to their distinct turnover times and stabilization mechanisms, POM and MAOM fractions have been extensively utilized to mechanistically investigate SOC stabilization and availability across contrasting land use practices in temperate zones (Schiedung et al., 2025).

The combination and interaction of POM and MAOM fractions can form complex but fundamental constituents of soil - soil aggregates. They are specifically formed by the interactions among organo-mineral complexes, microorganisms, and organic binding agents such as root hairs, fungal hyphae, and root exudates. It plays a critical role in the physical protection of SOM besides the chemical resistance of MAOM fraction (Totsche et al., 2018). Aggregation physically isolates portions of POM and microbial necromass from

microorganisms, effectively reducing their accessibility to microbial decomposition and thus increasing the overall SOC stabilization (Lavallee et al., 2020; Six et al., 1998). This means that microaggregates can contain both some POM fraction and a large amount of MAOM fraction (Spohn and Giani, 2011), which may be critical for coupled C-N-P cycling in the bulk soils, though the mechanistic understanding of their cycling is still limited, particularly the P.

1.3 Element stoichiometry as a tool for understanding biogeochemical cycling

The biogeochemical cycles of OC, N, and P are tightly coupled, meaning that soils with high OC stocks also typically store significant amounts of N and P, and vice versa. Such patterns have been clearly illustrated in stoichiometric studies showing consistent enrichments of N and P in SOM. The stoichiometry of C:N:P has been extensively explored across various soil components, including plant residues, microbial biomass, and SOM. Each component displays distinctive elemental ratios: microbial biomass commonly has a C:N ratio averaging around 9:1 (Cleveland and Liptzin, 2007), whereas plant-derived biomass typically exhibits much higher ratios, occasionally exceeding 100:1 (Cotrufo et al., 2019; Kirkby et al., 2011; Tipping et al., 2016), and highly variant between plants and organic fertilizers. The substrate stoichiometry can significantly influence the biogeochemical cycling processes of N (Schleuss et al., 2021). Therefore, due to distinct plant residue inputs and different decomposition rates and stabilization of OM driven by land uses, grasslands generally have a higher microbial biomass C:N ratio compared to cropland soils, likely reflecting microbial community composition (Li et al., 2024).

Interestingly, despite the significant variability observed in microbial and plant-derived OM, MAOM fraction in soils consistently maintains a relatively narrow C:N ratio of approximately 12:1 (Cotrufo et al., 2019). There are studies claiming the main reason is the consistent C:N ratio of resistant OM, while some assign this stability as the microbial immobilization of OC in biomass/necromass, which can subsequently bind to minerals and be physical protected within soil aggregates (Kögel-Knabner, 2008). In both cases, C:N ratio in the MAOM fraction serves as a valuable qualitative indicator of the OC stabilization (Cotrufo et al., 2019; Kirkby et al., 2011).

Similar patterns are evident in the stoichiometric relationships involving P. The OC:P ratio, especially the OC:OP ratio, is narrow in the MAOM fraction, generally averaging around 200:1 (Kirkby et al., 2011). In contrast, POM fractions show substantially greater variability, ranging widely from approximately 100:1 to over 6000:1 due to their dominant nature of undecomposed plant residues (Cleveland and Liptzin, 2007; Fanin et al., 2015; Spohn, 2020b). As the MAOM fraction is enriched with microbial biomass/necromass, this results in a OC:P ratio ranging from 23:1 to 100:1 (average approximately 60:1) in grassland and cropland soils (Cleveland and

Liptzin, 2007; Fanin et al., 2015; Griffiths et al., 2012; Heuck et al., 2015; Khan and Joergensen, 2019; Turner et al., 2013; Xu et al., 2013). These differences in OC:P ratios observed in POM and MAOM fractions directly reflect on the distinct ratios in different soil particle sizes, with finer sizes exhibiting lower OC:P ratios (Spohn, 2020b). In contrast to plant and microorganisms, monoester-orthophosphates and diester orthophosphates exhibit molar C:P ratios from approximately 1:1 to 11:1 (Condron et al., 2005). These contrasting patterns in OC:P ratios have increased interest in using elemental stoichiometry as an indicator to investigate OP stabilization and retention mechanisms (George et al., 2018). The interaction and combination of these components in mineral soils thereby result in molar OC:OP ratios of 728, 433 and 309 in temperate forest, temperate grassland and temperate cropland topsoils and 278, 218 and 185 in their respective subsoils (Spohn, 2020b).

Although Kirkby et al. (2011) and Spohn (2020b) emphasize the relatively stable OC:OP ratio in the MAOM fraction (compared with the significant variations observed among plant residues and microbial biomass) based on relatively constant C:P ratio in SOM, Williams and Steinbergs (1959) suggest that OP might be stabilized through direct associations with OC, independently of N. Their observations are supported by weaker correlations between OP and N compared to OC and N. These uncertainties, however, continue to limit mechanistic understandings of P cycling, particularly OP cycling, in relation to OC and N dynamics.

Overall, the strong stoichiometric coupling between OC, N, and P storage in temperate soils emphasizes their critical role in regulating soil fertility and ecosystem sustainability. Yet, unlike OC and N, the specific forms in which P is stored in soils are significantly influenced by land uses. Given the differences in stabilization and availability of various P forms, more detailed investigations are essential to better manage land uses for sustainable P utilization.

1.4 Stabilization processes of soil inorganic and organic phosphorus

In temperate zones, IP is primarily stabilized as orthophosphate (mainly as $H_2PO_4^-$ and HPO_4^{2-}) through interactions with mineral surfaces and OM, influenced strongly by environmental conditions such as soil pH, ionic strength, redox potential, and SOM contents (Fig. 1.1). Major stabilization processes include ligand exchange (forming inner-sphere complexation), electrostatic attraction (forming outer-sphere complexation), (re)precipitation, occlusion, metal bridging, and hydrogen bonding. Typically, IP stabilization predominantly occurs on Fe/Al (hydr)oxides and 1:1 phyllosilicates, whereas association with 2:1 phyllosilicates is widely regarded as less significant due to their lower specific surface areas, limited reactive sites, and relatively weak adsorption capacity (Strawn et al., 2019).

The occurrence of ligand exchange exhibits mineral-specific and pH-dependent behaviors (Strawn et al., 2019). The permanent negatively charged basal planes of 2:1 phyllosilicates, derived primarily from isomorphic substitution in tetrahedral and octahedral sheets, become positively charged at the weathered or frayed edges through the protonation of oxygen functional groups (hydroxylated surfaces forming Al-OH and Si-OH) under acidic conditions. These positively charged edges attract orthophosphate anions via ligand exchange, specifically, by replacing hydroxyl groups, forming relatively stable inner-sphere complexes. However, although lower pH enhances the formation of these complexes, such complexes are less frequent on 2:1 phyllosilicates compared to Fe/Al (hydr)oxides and 1:1 phyllosilicates due to limited mineral edge availability.

In contrast, due to the lack of extensive isomorphic substitution that confers a permanent surface charge, 1:1 phyllosilicates and Fe/Al (hydr)oxides exhibit extensive protonation and deprotonation, thus generating highly reactive mineral surfaces at various soil pH (Strawn et al., 2019). Consequently, in strongly weathered soils (e.g., Oxisol, Ultisol, Andosol) (Zech et al., 2022), abundant kaolinite and Fe (hydr)oxides with low pH show strong positive charges on mineral edges, strongly adsorbing to negatively charged orthophosphate through the dominant formation of inner-sphere complexes via ligand exchange. These interactions lead to persistent P retention that is relatively less reversible, although alterations in soil pH and ionic strength can still partially reverse these bonds (Fig. 1.1).

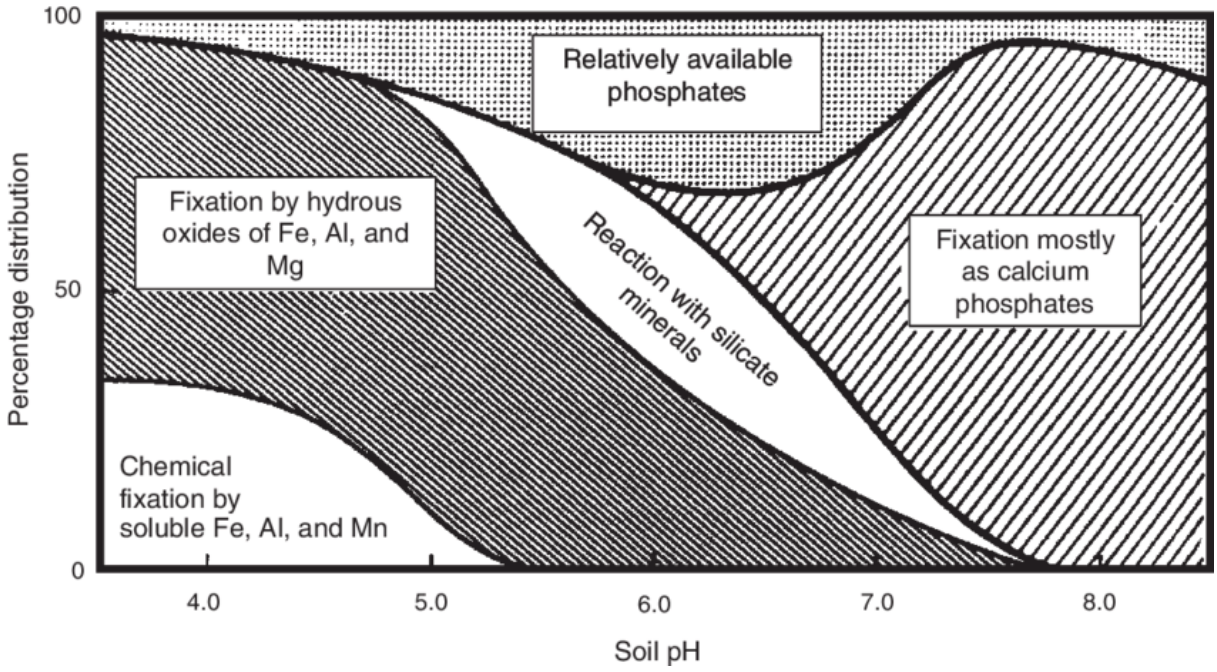

Fig. 1.1 The relationship between pH and fixation of phosphorus with different minerals (derived from Brady et al. (2008))

Orthophosphate may also adsorb to mineral surfaces through electrostatic attraction, referred to as outer-sphere complexes. Such outer-sphere complexes, characterized by weaker Coulombic interactions, are highly reversible and sensitive to soil solution conditions (pH and ionic strength) (Strawn et al., 2019). As Fe/Al (hydr)oxides can undergo extensive protonation and deprotonation, creating predominantly positive or negative surfaces, electrostatically adsorbed IP on these oxides is often considered a key source of plant-available P in soils with higher pH (close to the point of zero charges). 2:1 phyllosilicates with predominantly negatively charged basal planes typically favor cation adsorption, though edge protonation under acidic conditions can permit some orthophosphate adsorption as reversible outer-sphere complexes. Since the outer-sphere complexes do not disrupt the hydration sphere of orthophosphate, the weak Coulombic interactions allow for easier displacement by competing ions, making this P fraction readily available when soil ionic strength or pH changes.

In addition to the rapid adsorption of orthophosphate onto mineral surfaces via ligand exchange and electrostatic attraction, soluble orthophosphate can undergo (re)precipitation processes, interacting slowly with exchangeable and soluble cations (e.g., Fe^{3+}, Al^{3+}, Ca^{2+}) in soil matrix to form secondary phosphate minerals. This process depends strongly on both the pH and redox potential of the soil solution. Acidic conditions predominantly favor the precipitation of Fe/Al phosphate minerals, initially forming amorphous precipitates that gradually transition into crystalline phases, reducing phosphate availability. As crystallinity advances, phosphate solubility diminishes, making it barely available to plants. Under alkaline conditions (pH > 7.5), calcium-driven precipitation predominates. The precipitation of orthophosphate forming secondary minerals mostly occurs associated with Al/Fe (hydr)oxides and rarely occurs on the surfaces of 2:1 phyllosilicates.

As these phosphate minerals form the newly precipitated phases may incorporate phosphate into the crystal lattice of (hydr)oxides or become coated by subsequent mineral layers. Through repeated cycles of adsorption and precipitation, previously adsorbed phosphate becomes progressively occluded and locked within the soil matrix. This process, referred to as phosphate occlusion, physical and chemical isolation of phosphate within mineral structures, renders phosphate far less available for plant use. The occlusion of phosphate with 2:1 phyllosilicate is much less common than (hydr)oxides due to the dominance of their non-reactive basal planes and limited recrystallization processes.

Organic matter contributes additional adsorption sites, primarily via negatively charged functional groups such as carboxylic and phenolic groups and higher specific surface areas. In acidic soils, due to the dissociation of protons from functional groups, particularly carboxylic and phenolic functional groups, the surface of OM is mostly negatively charged. The polyvalent cations, especially Ca^{2+}, Mg^{2+}, Al^{3+}, and Fe^{3+}, can bridge negatively charged organic functional

groups with negatively charged orthophosphate through electrostatic forces (Coulombic forces), with occasional ligand exchange when hydroxyl groups coordinate these cations. In addition, hydrogen bonding between orthophosphate and positively charged amine or hydroxyl groups of OM can occur, though these interactions are even weaker than electrostatic attractions. Nonetheless, the direct OM-bound orthophosphate fraction generally constitutes less than 10% of IP in acidic mineral soils with low/moderate OM content. Biological processes, particularly microbial uptake, also temporarily immobilize IP in microbial biomass. However, microbial contributions to total IP pools are typically few (Fig. 1.2).

In contrast to IP, organic phosphorus is stabilized primarily through ligand exchange, forming inner-sphere complexes on charged mineral surfaces (Eusterhues et al., 2023; Spohn, 2024) and assimilation/immobilization in microorganisms (Fig. 1.2). Additional minor stabilization mechanisms include electrostatic attraction, mineral surface precipitation, and physical protection within soil aggregates. The formation of inner-sphere complexes via ligand exchange is generally considered primarily occur on (hydr)oxides surfaces, as both phosphate diester groups (e.g., extracellular polymeric substances) (Omoike and Chorover, 2006) and phosphate monoesters have higher affinity to adsorb to (hydr)oxides compared to phyllosilicate minerals. Among phyllosilicates, 1:1 phyllosilicates typically adsorb OP more effectively than 2:1 phyllosilicates, though these interactions remain strongly influenced by soil pH and ionic strength (Spohn, 2024).

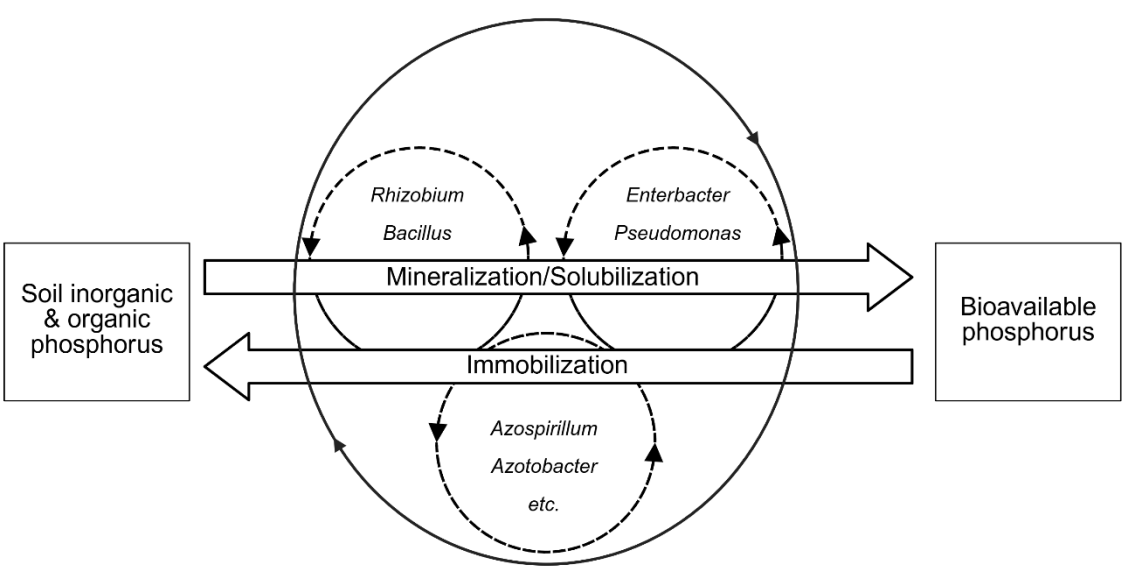

Fig. 1.2 Phosphorus immobilization and mobilization by microorganisms in soils (derived from Khan et al. (2009))

Microorganisms significantly contribute to OP stabilization, with a lower C:N ratio favoring higher OP stability (Sun et al., 2022), primarily as orthophosphate diester, more specifically, as nucleic acids (Condron et al., 2005). In addition, microbial extracellular polymeric

substances can stabilize OP via ligand exchange with mineral surfaces, especially Fe/Al (hydr)oxides (Fang et al., 2017; Omoike and Chorover, 2006), albeit generally with lower affinity to adsorb to minerals compared to orthophosphate monoesters (Stewart and Tiessen, 1987). Orthophosphate monoesters constitute the largest OP group in temperate soils (Darch et al., 2014; Stutter et al., 2015), with *myo*-inositol phosphate being the dominant monoester group primarily derived from plant residues and those plant-based fertilizers (e.g., manure) (Condron et al., 2005). Compounds with multiple phosphate groups, such as *myo*-inositol hexaphosphate, exhibit greater stability than IP or other OP compounds with fewer phosphate groups through chelation with metal cations (Gerke, 2015) and multi-dentate ligand exchange reactions on mineral surfaces (Spohn, 2024; Strawn et al., 2019). *Myo*-inositol hexaphosphate is suspected to be able to bind to both minerals and organic compounds that are less strong in competing for binding sites on mineral surfaces (Spohn, 2024), though the detailed mechanisms are still unknown.

Due to their distinct stabilization mechanisms and availability, IP and OP differentially affect soil P turnover and ecosystem availability in temperate zones. Continued high consumption of finite phosphate rock resources (in the form of IP) globally to produce P fertilizers, driven by the increasing food demand, has sparked an intense debate on potential looming P scarcity or price spikes (Cordell and White, 2011; Mew et al., 2023; Scholz et al., 2025). Concurrently, soil P stocks loss (Alt et al., 2011; Hedley et al., 1982; Kopittke et al., 2017) and soil degradation (Borrelli et al., 2017) have been exacerbated by natural vegetation land use changes toward cropland to meet growing food demands, further contributing to unsustainable P cycling. In response, efforts are required to mechanistic understanding of their respective behavior in soils associated with OC and N for sustainable P management (Sulieman and Mühling, 2021).

1.5 Nano-scale secondary ion mass spectrometry (NanoSIMS) as a tool for organo-mineral interaction studies

Nano-scale secondary ion mass spectrometry (NanoSIMS) enables a resolution of 50-100 nm to observe element distribution in intact soil structures and their individual associated components, including microaggregates, Fe/Al (hydr)oxides, microorganisms, and POM surfaces or macroaggregate at the relevant process scale (Goss and Oliver, 2023). Previous NanoSIMS studies in soil science have put emphasis on investigating SOM dynamics and element cycling for better mechanistic understanding of the organo-mineral interactions (Li et al., 2023) and the dynamics of plant-soil interactions, including rhizosphere processes (Vidal et al., 2021).

Nevertheless, NanoSIMS has several limitations. For example, the NanoSIMS analysis requires very small sample sizes, complicating work with heterogeneous soils. The complex and meticulous sample preparation process is time-intensive and impacts on the precision and reproducibility of results. Isobaric interference, dead-time corrections, matrix effects, and surface sensitivity further complicate accurate isotopic quantification. In addition, the quantification and differentiation of element forms are still challenging (Li et al., 2016), including OP and IP (Kruse et al., 2015; Li et al., 2023), despite their distinct stabilization and availability behavior in soils. Given the critical role of OP in sustainable P utilization and its resilience against soil degradation (Sulieman and Mühling, 2021), a deeper mechanistic understanding of OP interactions with SOM, soil microorganisms, and active mineral surfaces is required (George et al., 2018).

1.6 Silicate mineral weathering as a potential strategy for nutrient supply and carbon sequestration under climate change

Silicate rock powder application (primary ERW materials) is an ancient practice as a soil improver for agricultural productivity (Leonardos et al., 1987; Van Straaten, 2007). The basalt powder has been proved to be profitable for rejuvenating tropical soils in Brazil (d'Hotman and Villiers, 1961; Leonardos, 1973) and has also been recommended for fertilizing nutrient-poor soils in Germany (Gerth, 1939; Hilf, 1938; Larson et al., 1938) by providing a serious of nutrients including Ca, magnesium (Mg), sodium (Na), sulfur (S), P, potassium (K) and other micronutrients. A recent review has confirmed the general benefits of silicate rock powder in increasing crop productivity and improving soil health, but their performances are constrained by soil types, plant species, rock/mineral types, rock particle sizes, and application amounts (Swoboda et al., 2022).

In facing the escalating climate crisis, fine silicate rock powder application in soils has emerged as a promising strategy for atmospheric carbon dioxide (CO_2) removal (CDR) as inorganic carbon (IC) besides its benefits on improving soil nutrients and health, which is shortly called enhanced rock weathering (ERW). Since it was initially proposed in 1990 as a potential means to mitigate greenhouse effect (Seifritz, 1990), ERW has gained substantial attention over recent decades as a potential strategy for CO_2 sequestration worldwide (Beerling et al., 2020; Buss et al., 2024a; Buss et al., 2024b; Hartmann et al., 2013; Kantola et al., 2017; Kelland et al., 2020; Köhler et al., 2010; Schuiling and Krijgsman, 2006; Sokol et al., 2024; Xu et al., 2024). This method involves applying finely ground calcium (Ca) and magnesium (Mg)-rich silicate mineral powders to soils, which accelerates the neutralization of H^+ derived from carbonic acid dissociation during silicate mineral dissolution (Oelkers et al., 2018). This results in an increased dissolved inorganic carbon (DIC) concentration in soil solution as bicarbonate and releases soluble ions (e.g., Ca^{2+} and Mg^{2+}), which can be transported to aquatic systems

for long-term carbon sequestration (Clarkson et al., 2024; Hasemer et al., 2024; Oelkers et al., 2018). Under alkaline conditions (Fig. 1.3), these ions can further precipitate with DIC in the form of Ca/Mg carbonates in the soil (SIC) or aquatic systems (Clarkson et al., 2024; Hasemer et al., 2024).

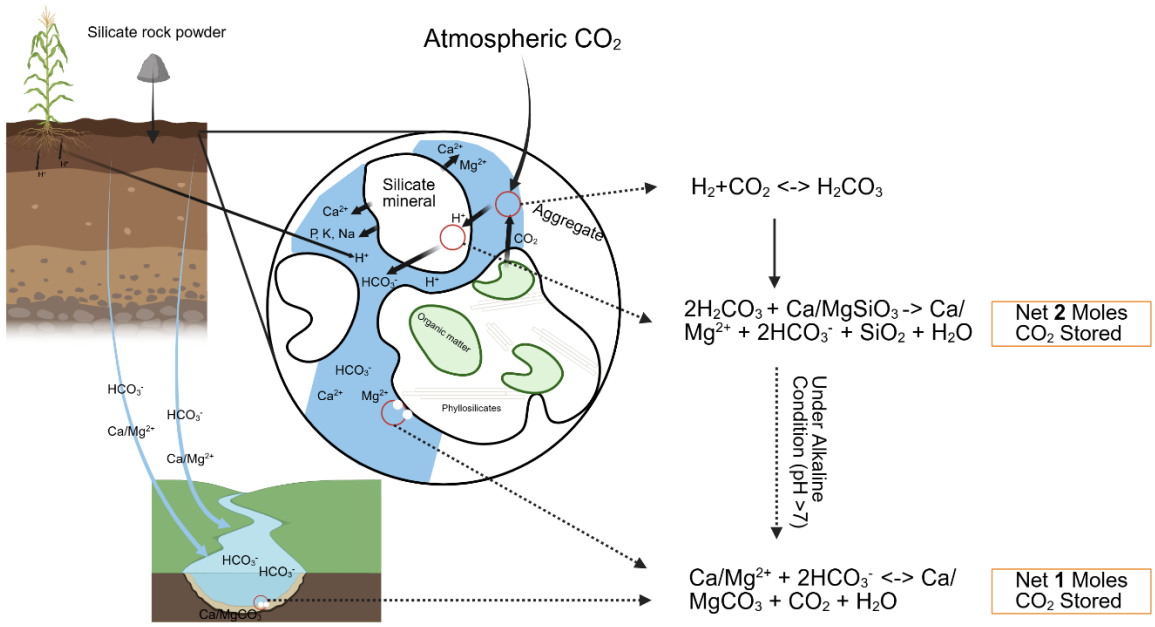

Fig. 1.3 The inorganic carbon pathway for carbon dioxide removal associated with ERW.

In general, those Ca and Mg enriched silicate minerals with isolated tetrahedra structure/chains structure are all potential options, including basalt (Beerling et al., 2025; Buss et al., 2024a; Haque et al., 2023), olivine (Amann et al., 2020; Dietzen et al., 2018; te Pas et al., 2023) and wollastonite (Haque et al., 2020; Haque et al., 2019; te Pas et al., 2023; Xu et al., 2024), as well as those industrial by-products including steel slag (Beerling et al., 2020; Buckingham and Henderson, 2024; Xu and Reinhard, 2025), mining tailings (Power et al., 2020; Power et al., 2023), fly ash and other construction waste (Beerling et al., 2020). Among various silicate minerals, basalt, as an abundant, cost-effective and fast-weathering rock enriched with olivine, is regarded as particularly suitable for large-scale ERW applications (Beerling et al., 2025; Beerling et al., 2020; Buss et al., 2024b).

The soil acidity correction by silicate minerals is regarded as one of the benefits of ERW. The H^+ neutralization and supplying base cations during the fast weathering of Ca/Mg-rich minerals can increase soil pH to different degrees, depending on the weathering stage of minerals and mineral types (Beerling et al., 2025). On the one hand, the increasing soil pH, especially in those slightly acid cropland soils in tropical and temperate zones (Levy et al., 2024), can directly enhance soil nutrient availability and indirectly release more nutrients by accelerating the solubilization of SOM, as most crops requiring optimal pH around 6.5 - 7. On the other

hand, the induced rising pH in the soil solution may affect SOC pools, as evidenced by SOC losses observed in soils treated with lime (Wang and Kuzyakov, 2024). The SOM stabilization in the pH range optimal for crops is relatively weaker due to the deprotonation of Fe oxides and SOM, which leads to the limited formation of stable inner-sphere complexes (Strawn et al., 2019). Previous studies have found that rising pH can stimulate microbial and enzymatic activities (Wang and Kuzyakov, 2024; Zhang et al., 2020) and increase nutrient availability (Kantola et al., 2017), potentially accelerating SOM decomposition and leading to SOC losses. The lime-induced SOM losses are particularly significant in acidic and slightly acidic soils. Extrapolated from this, the increased pH caused by ERW materials may also affect soil OC in the long term. Yet, the magnitude and long-term persistence of these effects remain uncertain, especially given the variability in the weathering stages of ERW materials (Beerling et al., 2025; Buss et al., 2024a; Vicca et al., 2022).

In addition to alkalinity effects, recent studies have reported positive (Bi et al., 2024; Buss et al., 2024a; Xu et al., 2024), neutral (Bucka et al., 2024; Sokol et al., 2024), and negative effects (Klemme et al., 2022) of ERW materials on SOC accrual. Theoretically, ERW can enhance carbon sequestration by promoting the formation of mineral-associated organic matter (MAOM), driven by the release of reactive secondary minerals and facilitating cation bridging during silicate mineral weathering, which has been observed in recent studies using fresh wollastonite (Xu et al., 2024). In contrast, a field trial applying meta-basalt to calcareous soils reported reduced MAOM-C, attributed to decreased active microbial biomass associated with ERW (Sokol et al., 2024). However, previous studies used only fresh ERW materials, which typically have a lower specific surface area and less reactive sites. Thus, the net carbon sequestration potential of ERW materials at more advanced weathering stages remains uncertain. In addition, OM coating/aggregation on mineral surfaces and organic acid released during OM decomposition can significantly influence primary/secondary mineral weathering (Drever and Stillings, 1997; Ritschel et al., 2023). Current ERW models, which primarily rely on theoretical oxide dissolution kinetics, may not adequately capture these complex interactions between OM dynamics and mineral dissolution processes. Thus, addressing these uncertainties is essential to optimize the implementation of ERW and accurately estimate its long-term carbon sequestration potential. The fact that all recent studies focus on fresh ERW materials, overlooking net C sequestration potential as weathering progresses, leads to an underestimation of ERW on CDR in the long term. Current ERW models mainly estimate IC based on theoretical elemental oxide compositions and dissolution kinetics of minerals (Beerling et al., 2025; Beerling et al., 2020; Renforth, 2019) and rarely address how ERW influences OC pool at different weathering stages, which is the biggest and primary C pool in terrestrial ecosystems. The dynamic interaction between IC and OC pools with the weathering

processes is also unknown, these gaps further hinder the accurate modeling and sustainable management of carbon associated with ERW.

Though recent researchers have started to realize that soil bio-processes may drive the performance of ERW and can be constricted by soil types, rock/mineral types, rock particle sizes, and application amounts, hardly any studies realize that natural soils continuously receive new OM inputs from plant residues, animals and anthropogenic organic fertilizers. The overlook of these constant new OM inputs makes it impossible to assess turnover and cycling of C and makes it essential when assessing the impacts of ERW on carbon sequestration across different ecosystems. Limited studies (Kelland et al., 2020; Xu et al., 2024) offered some preliminary insights into how plant residue inputs may influence ERW-driven changes in SOC contents, they have not yet clarified the effects of ERW on the fate of both native and new OC with the weathering progresses. Consequently, the mechanistic understanding of how these new and native OC pools interact with ERW-induced IC pools remains incomplete, which makes the comprehensive evaluation of long-term C sequestration by ERW impossible.

Besides the lack of mechanistic understanding of how the ERC-derived IC and OC interact over time, some preliminary life-cycle assessments of ERW strategy give some case studies on the efficiency of applying ERW materials in croplands (Beerling et al., 2025; Lefebvre et al., 2019). The low transporting efficiency determines that the transporting of these materials from the quarry to the field can release a significant amount of CO_2, particularly considering the basalt mining and grinding in the quarry. This is also one of the biggest concerns when ERW was proposed in 1990 as the means of CDR (Seifritz, 1990). A recent study by Beerling et al. (2025) has tried to estimate the capability of a large-scale application of basalt in the USA and emphasize its long-term promise for CDR domestically associated with basalt quarry plants, without considering the SOC pools. Therefore, unlike other chemical fertilizers, ERW for CDR may be limited by its high cost for transportation, though this may only be used once over decades considering the time it would take for weathering.

In Germany, the mean value of pH of cropland soils is 6.1, and over 50% of the sites with crop rotations including potatoes, winter rye, spring oats, or maize have soils with low or very low pH (Müller et al., 2022). The state of Bavaria has one of the biggest croplands and grassland areas in Germany, which is covered by typical temperate soils with the dominant of weathering minerals including Cambisol, Luvisol and Fluvisol. Most of the cropland soils in Bavaria have pH ranging from 5.5 to 6.5 (Müller et al., 2022). This pH range is suitable for the application of ERW materials for soil acidity correction purposes (Clarkson et al., 2024), as they can increase those slightly acidic soils to the most optimal pH range, allowing for maintaining optimal nutrient uptake and avoiding toxicity from trace metals. Basalt reserves estimated by the Federal Institute for Geoscience and Natural Resources in Germany are approximately 150 million

tonnes (https://www.bgr.bund.de), potentially allowing for a large-scale domestic application in croplands to mitigate escalating climate change. The higher cropland coverage in Bavaria, the abundant basalt reserves, and the necessity for soil acidic correction may be suitable for the application of basalt, considering its short transportation distance and efficient spreading techniques.

1.7 Objectives and approaches

The main objective of this publication-based thesis is to deepen the mechanistic understanding of the distinct impacts of land use and soil development processes on C, N and P stocks and cycling in Bavaria landscape, particularly the OC and OP interaction processes within SOM, and their association with minerals. To offset the degraded cropland soils C stock, ERW is evaluated as a solution for maintaining nutrients levels, correcting soil acidity and enhancing carbon sequestration capacity.

To achieve these objectives, the detailed studies and their corresponding approaches were listed below:

1.7.1 Distinct impact of land use and soil development processes on coupled biogeochemical cycling of C, N and P in a temperate hillslope-flood plain system

To better evaluate the C, N and P stocks and their stability in temperate soils, this study examined a temperate hillslope-flood plain system in Bavaria Forest regions, with typical temperate soil types, to answer the following questions:

- How do land uses and soil development processes shape the stocks of OC, N, and P in topsoil and subsoil?
- What are the drivers underlying TP partitioning (IP vs. OP) and stoichiometric correlations of OC:TN and OC:OP across different soil fractions?
- What are the implications of these stoichiometric correlations in soil different fractions for understanding OP stabilization mechanisms and cycling?

To differentiate land use and soil development factors, this study took advantage of investigating a periglacial loess loam-affected slope-flood plain system in a granitic region of the Bavarian Forest with documented historical land use and geomorphological information. This was a representative slope-flood plain system in the low mountain range of the temperate zone.

This study analyzed bulk soils for OC, TN, TP, IP, and OP contents and stocks in soils under long-term cropland and grassland use, and under the influence of colluvium and alluvium

sedimentation. The ^{15}N signature and ^{13}C solid-state nuclear magnetic resonance (NMR) spectroscopy gave detailed information on the sources and retention ability of SOM. Further physical fractionation and stoichiometric analysis in fine (<20 μm) and coarse (>20 μm) soil fractions reflected the distribution and enrichment of SOM in these fractions, which were necessary for revealing their stoichiometric correlation and stabilization status to recognize and differentiate pathways of OP cycling in the MAOM fraction.

1.7.2 Phyllosilicates and their associated OM determine the retention and availability of P in temperate soils

In the context of general biogeochemical cycling of OC, TN and different forms of P in these regions, to better understand the stabilization processes and availability of different forms of P in the context of OC and N cycling for sustainable P use for maximizing agricultural productivity. This study aimed at answering the following questions:

- What is the role of phyllosilicate in retaining different forms of P in temperate soils?
- Are there any preferences for different forms of P to associate with different minerals?
- What can the spatial distribution of these P forms on mineral surfaces imply for soil management under contrast land uses?

To accomplish these objectives, four fine soil samples (< 20 μm fraction) from temperate regions representing four common temperate soil types were selected. These soils exhibited moderate degrees of weathering, similar mineral compositions, but distinct differences in OC content, P partitioning, and P availability. Specifically, Cambisols and Luvisols were common soil types found in temperate humid environments, while Phaeozems typically occurred in transitional zones adjacent to humid forests (Nortcliff, 2009; Zech et al., 2022). Fluvisols, abundant in periodically flooded temperate landscapes, typical had a substantial P storage capacity (Nortcliff, 2009; Zech et al., 2022).

This study combined NanoSIMS with an unsupervised segmentation method to investigate the micro-scale distribution of IP and OP on soil microaggregates. Four P reference standards representative of temperate soils were employed: *myo*-inositol hexaphosphate (a major OP compound), *Bacillus subtilis* (providing a complex suite of diesters and polyphosphates alongside orthophosphate), aluminum phosphate and iron phosphate (common IP forms in acidic environments). By correlating them with bulk physicochemical data from Study I, this work was able to provide mechanistic understanding of how IP and OP compounds interact with specific minerals and OM to delineate P retention and availability pathways in these temperate systems.

1.5.3 Balance organic and inorganic carbon in enhanced rock weathering: Implication for carbon sequestration

ERW is regarded as a viable CDR strategy, owing to its ability to promote IC sequestration through carbonic-acid reaction with silicate minerals. Yet, its impact on SOC remains poorly understood, since ERW both increases IC storage and raises soil pH via proton neutralization. To quantify the net carbon balance of ERW, this study performed a controlled microcosm study using three basalt materials and applied them to a temperate Cambisol topsoil derived from Study I. These treatments mimicked successive stages of basalt weathering, with included ^{13}C-labeled straw simulating continuous plant-residue inputs. This study aimed to answer the following key questions:

- Which mechanisms drive C stabilization and losses in soils applied with basalt materials at different weathering stages?
- What are the long-term implications of basalt application for soil C sequestration?
- How do interactions between OC and IC pools influence the overall effectiveness of ERW as a climate mitigation strategy?

To address these questions, this study monitored C fluxes within atmosphere-soil-effluent system over 6 months, measuring the CO_2, SOC, SIC, and dissolved organic and inorganic carbon in the effluent. Meanwhile, to elucidate which factors determine the change of C fluxes, the physicochemical properties of soils were measured. By providing a complete C fluxes assessment during 6-month incubation, this study aimed to clarify the net impacts of ERW on the cycling and interactions of OC and IC at different weathering stages.

2 Material and Methods

2.1 Study site and soil description

2.1.1 Study site description (Study I)

The research site is located near Süssenbach (49°06′12″ N, 12°21′37″ E) in the Falkensteiner Vorwald region, part of the Bavarian Forest in southeastern Germany. The climate there is typical temperate, with a mean annual temperature of 8.9 °C and mean annual precipitation of 875 mm. The primary parent material is saprolite derived from granite (Regensburger Kristallgranit I), as mapped in the digital geological map 1:25,000 (Umwelt, 2024). This granitic substrate has been modified by loess deposits and slope-derived colluvial sediments dating back to the Late Pleistocene period (Völkel, 1995).

The site includes an NNW-facing slope, and an adjoining flood plain connected to the Otterbach stream (referred to as “Süssenbach” in older cartographic sources; see Fig. 2.1). For slope site analysis, the slope is divided into upper, middle, and lower parts. These divisions are applied solely for location reference and do not correspond to specific geomorphological characteristics of a slope profile. A detailed description of the slope can be found in Study I, Table S2.

Documented historical maps indicate that deforestation took place around 1950, at which point both cropland and grassland were established on the slope. Current grassland use areas are temporarily cultivated, as evidenced by the presence of Ap horizons (Fig. 2.1). Meanwhile, the flood plain, which has functioned as unmanaged natural grassland since at least 1890, transitioned to regularly managed grassland since approximately 1980 (Fig. 2.1).

The Otterbach, a second-order tributary flowing into the Danube at Sulzbach (Opf.), lies at an elevation of 473 meters above sea level and was in a relatively natural state until it was managed and channelized in 1980. According to hydrological records from the Bayerisches Landesamt für Umwelt (2023), its mean annual discharge between 1957 and 2013 is 0.833 m^3 s^{-1}, with annual extremes ranging from 0.156 m^3 s^{-1} and 11 m^3 s^{-1}.

In terms of soil classification (Schad and Dondeyne, 2016), most of the slope soils are characterized as Cambisols, except for the lower grassland part, where a Luvisol is found. On the flood plain, two contrasting soils are identified: Fluvisol (FPF) and Phaeozem (FPP) (Fig. 2.1). Detailed descriptions of these soil profiles can be found in the Supplementary Material of Study I.

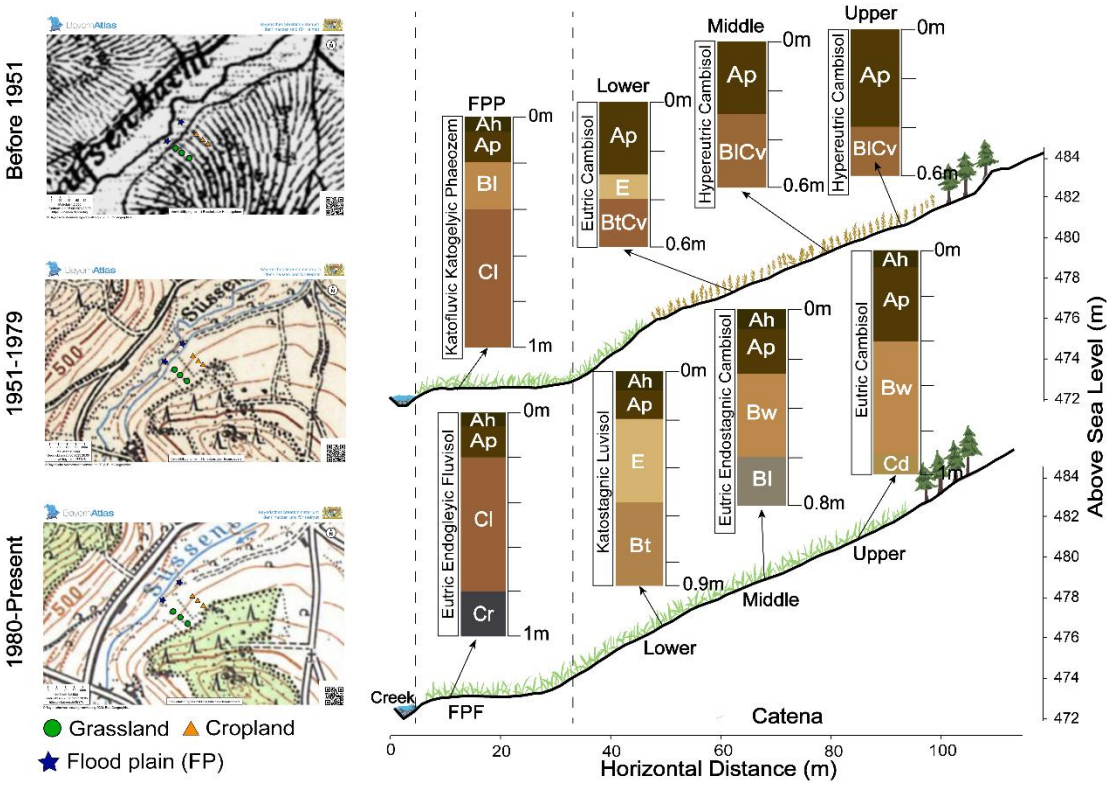

Fig. 2.1 Historic maps (BayernAtlas, Bayerisches Staatsministerium der Finanzen und für Heimat, 2023) and schematic graph of the study site Süssenbach. 'Upper', 'Middle', 'Lower', 'FPF', and 'FPP' means the upper, middle, and lower parts of the slope, Fluvisol, and Phaeozem in the flood plain, respectively. (Figure is taken from Study I).

2.1.2 Soil description (Study I, II, III)

The cropland situated along the slope has been subjected to intensive farming practices, including regular organic fertilization, for more than three decades. In the upper and middle parts of the slope, the Ap horizon is characterized by a silt loam texture, transitioning into a loam texture within the deeper BC horizon. Soil pH in these areas consistently exceeds 5.8 or 6.1, corresponding to base saturation levels above 50% and 80%, respectively. Organic carbon concentrations surpass 1% within the top 50 cm of the profile. Based on these parameters, the World Reference Base for Soil Resources (WRB) classifies these upper and middle slope soils as Hypereutric Cambisols (Siltic, Aric, Humic). On the lower parts of the slope, however, the soil exhibits lower pH values in the B horizon and a distinct lithic discontinuity, leading to its classification as a Eutric Cambisol (Siltic, Aric, Humic, Epiraptic).

On the upper slope of grassland, the soil maintains a consistent loam texture and features a well-developed cambic horizon. With a pH consistently above 4.5 and the presence of transported material in the top 40 cm, this soil is identified as a Eutric Cambisol (Pantoloamic, Humic, Transportic). In the middle slope of grassland, signs of earlier cultivation are visible in the form of a relic Ap horizon, while redoximorphic features in the subsoil suggest intermittent

water saturation. Accordingly, this profile is classified as an Eutric Endostagnic Cambisol (Pantoloamic, Aric, Humic). In the lower slope part of grassland, loess deposits and redoximorphic features were observed in the deeper horizons. These indicate clay illuviation and periodic saturation, supporting its classification as a Katostagnic Luvisol (Pantoloamic, Differentic, Eutric, Humic, Endoraptic).

Soils in the flood plain exhibit clear differences. Under cropland used slope, the soil shows pronounced gleyic features, with a loam texture at the surface giving way to loamy sand in the subsoil. Sedimentation structures are evident at around 40 cm depth. The presence of a mollic horizon warrants its classification as a Katofluvic Katogelyic Phaeozem (Epiloamic, Katoarenic, Humic, Katogleyic). In contrast, the grassland soil in the flood plain, primarily shaped by alluvial sediment deposition and lacking a mollic horizon, is classified as a Eutric Endogleyic Fluvisol (Loamic, Humic).

Plant species composition also varies by land use. Grasslands in the flood plain were primarily composed of *Alopecurus pratensis*, *Anthoxanthum odoratum*, and *Veronica chamaedrys*. On the slope grasslands, dominant species shift to *Dactylis glomerata*, *Alopecurus pratensis*, and *Plantago lanceolata*. Recent crop rotations on the cropland have included oat (*Avena sativa*), triticale (*Tritico secale*), winter barley (*Hordeum vulgare*), and rye (*Secale cereale*) (Martínez-Cuesta et al., 2025).

2.2 Incubation experiment setup and sampling (Study III)

Approximately 250 g of dried cropland soil (< 2 mm) was incubated in microcosms (5 cm in height, 8 cm internal diameter) for six months in a dark, open system at a constant room temperature of 25 °C. The soil was sourced from the Ap horizon of the cropland on the slope of Süssenbach (Fig. 2.1, taken from Study I).

Basalt and weathered basalt materials were sourced from the Zeilberg quarry (50°11’46”N, 10°40’27”E) managed by Basalt-Actien-Gesellschaft, Germany. Detailed properties of these materials and X-ray diffraction (XRD) results can be found in Lei et al. (2025b).

The ^{13}C-labelled rice straw was homogenized by ball-grinding for 1.5 min at 25 Hz after cooling with liquid nitrogen. It was mixed at 0.8% by weight with soil and treatments. Straw had OC content at 400 mg/kg with a C/N ratio of 14 and a ^{13}C enrichment of 238‰. Additional information of straw is shown in Lei et al. (2025b).

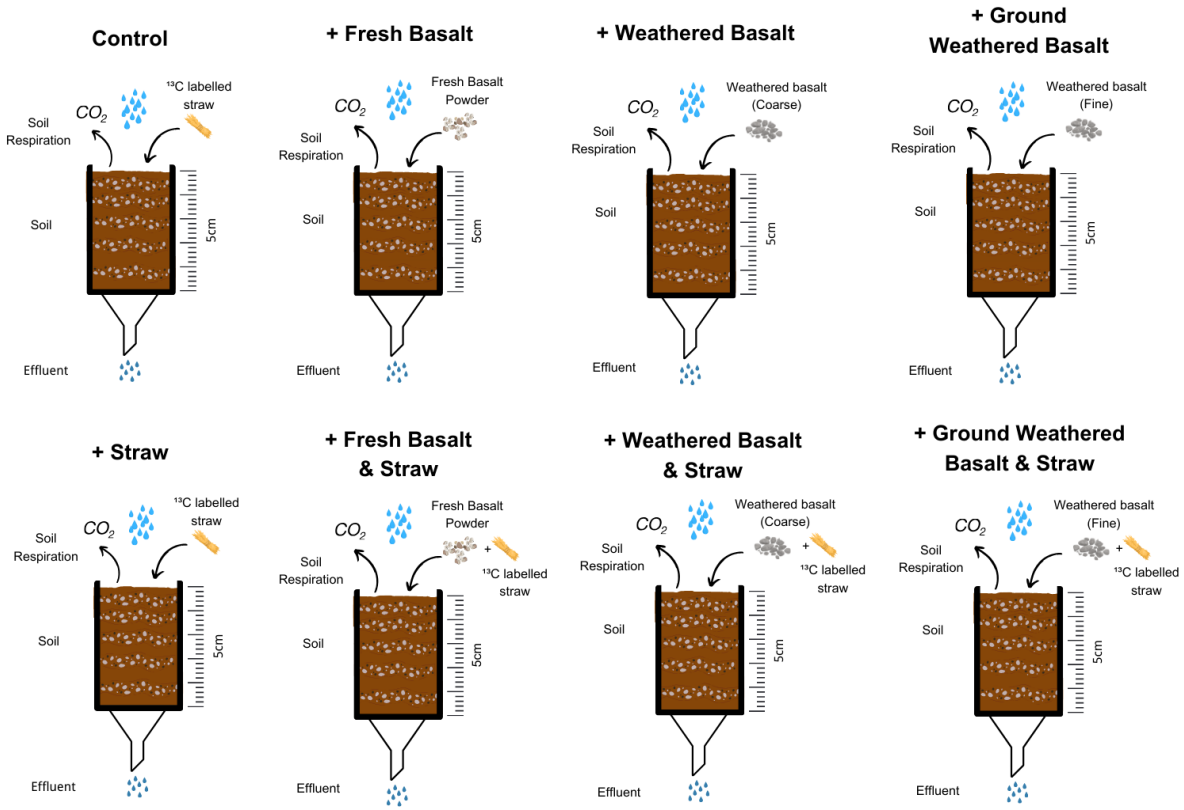

Fig. 2.2 The schematic graph of incubation experiment of Study III.

The dosage of treatments is 5 kg/m^2 at 10 cm depth (equal to 4%). The microcosm experiment (Fig. 2.2) included one control and 5 treatments: + F. Basalt (96% soil, 4% fresh basalt), + W. Basalt (96% soil, 4% weathered basalt), + G.W. Basalt (96% soil, 4% ground weathered basalt), + Straw (99.2% soil, 0.8% rice straw), + F. Basalt & Straw (95.2% soil, 0.8% rice straw, 4% fresh basalt), + W. Basalt & Straw (95.2% soil, 0.8% rice straw, 4% weathered basalt), and + G.W. Basalt & Straw (95.2% soil, 0.8% rice straw, 4% ground weathered basalt). Each of them had five replicates in a randomized block design. Corrections were made for the dilution effect caused by the additional treatments (4%).

2.3 Soil physicochemical analyses (Study I, II, III)

2.3.1 Soil pH (Study I, II, III)

For pH analysis, ~5 g of soil was mixed at a 1:2.5 (w/v) ratio with 0.01 M l^{-1} calcium chloride solution and measured with the pH meter (Seven Easy pH, Mettler-Toledo, Switzerland).

2.3.2 Soil particle size distribution (Study I, III)

For soil samples taken from Study I, soils with an OC content higher than 15 mg g^{-1} were dispersed with 0.025M $Na_4P_2O_7$ before OM removal with 30% H_2O_2. Approximately 20 g of dry soil was then moistened with 25 ml 0.1M $Na_4P_2O_7$, followed by the addition of 200 ml of water. The mixture was dispersed in an ultrasonic bath for 10 minutes and shaken overnight. The soil

was separated into sand (2000-63 μm), silt (63-2 μm), and clay (<2 μm) particles using the Koehn pipette and sieves. Detailed data can be found in Lei et al. (2025a).

For soil samples taken from Study III, ~ 10 g of soil was moistened and dispersed using 0.05 M l^{-1} $Na_4P_2O_7$ with an energy input of 450 J l^{-1}. Sand-size fractions (>63 μm) were separated by wet sieving, while the < 63 μm fraction was further dispersed overnight and analyzed using X-ray sedigraph (SediGraph® III Plus, Micromeritics, USA). Detailed data can be found in Lei et al. (2025b).

2.3.3 Specific surface area analysis (Study III)

Soil samples taken from the middle section of the microcosms were oven-dried at 40 °C, with macroaggregates gently broken down and sieved to <2 mm for the analysis of Brunauer-Emmett-Teller (BET) surface areas (referred to as SSA). The SSA was measured using nitrogen (N_2) adsorption at 77 K following the BET method (Brunauer et al., 1938) by the gas adsorption analyzer (AUTOSORB I, Quantachrome, USA). Detailed data can be found Lei et al. (2025b).

2.3.4 Soil effective cation exchange capacity and exchangeable cations analysis (Study III)

For exchangeable cations and eCEC, the cobalt hexamine method was employed for its repeatability in slightly acidic soils (Nel et al., 2023). Detailed data can be found in Lei et al. (2025b).

2.3.5 Soil total element analysis (Study I, III)

Total P, as well as other total elements including sodium (Na), calcium (Ca), magnesium (Mg), aluminum (Al), nickel (Ni) and cadmium (Cd) were determined by a mixture of concentrated $HClO_4$-HNO_3-HF-HCl method (Page, 1982). Detailed data can be found in Lei et al. (2025a).

2.3.6 TC, SOC, SIC, $\delta^{13}C$ and $\delta^{15}N$ analysis (Study I, II, III)

The TC, SOC, SIC, $\delta^{13}C$ (‰ V-PDB) and $\delta^{15}N$ (‰ N_2) contents of the soil were measured via an isotopic ratio mass spectrometer (IRMS, Delta V Advantage, Thermo Fisher, Dreieich, Germany) coupled with an Elemental Analyzer (Euro EA, Eurovector, Milan, Italy). Carbonates were removed from soils using 2 N HCl for SOC content and $\delta^{13}C$ measurements (Midwood and Boutton, 1998), while non-acid-treated soils were analyzed for TC, $\delta^{13}C$ and $\delta^{15}N$ contents. SIC content is calculated by subtraction between TC and SOC contents.

The proportion of straw-derived OC stabilized (f) in the soil was calculated using the equation:

$$f = \frac{\delta_t - \delta_s}{\delta_r - \delta_s}$$

where δ_t = $\delta^{13}C$ of the soil with additional treatments after carbonate removal, δ_s = $\delta^{13}C$ of their respective control soils after carbonate removal; δ_r = $\delta^{13}C$ of the added treatments. Detailed data can be found in Lei et al. (2025b).

2.3.7 Organic phosphorus (OP), inorganic phosphorus (IP) and available phosphorus analysis (Study I, II)

In Study I, II, both OP and IP content of the bulk soil and soil fractions was determined through a modified sulfuric acid method (Walker and Adams, 1958). Briefly, the OP content was calculated as the difference in orthophosphate determined from pre-muffle furnace ignited soil (550 °C, 1 h) and non-ignited soil after extraction with 0.5 M H_2SO_4 for 16 h. The non-ignited extracts represented the IP content. All extracts were subsequently filtered through Munktell 131 filter paper (<5 µm) (Ahlstrom Munksjo) for further analysis by inductively coupled plasma optical emission spectroscopy (ICP-OES, Varian Vista-Pro, CCD).

In Study II, ~ 2 g soil (bulk soil and fine fraction soil) was mixed with 40 ml sodium bicarbonate solution (0.5 M) to extract available P. The extractants were centrifuged and filtered through PES syringe filter (<0.45µm) (Berrytec® GmbH) for further analysis by ICP-OES (Olsen, 1954).

2.3.8 Particle size fractionation (Study I, II, III)

A simple particle size fractionation method was applied to fractionate bulk soil into a fine fraction (<20 µm) and a coarse fraction (20-2000 µm) with distinct SOM turnover times (Just et al. 2021). Detailed data can be found in Lei et al. (2025a, 2025b).

2.3.9 Mineral characterization (Study II, III)

In Study II, soil samples were taken from Süssenbach topsoil, while in Study III, the basalt and weathered basalt were analyzed. Clay size particles were sieved out by using the Koehn pipette and sieves. Soils were dispersed with 0.025M $Na_4P_2O_7$ prior to OM removal with 30% H_2O_2. Subsequently, approximately 20 g of air-dry soil/basalt material was moistened with 25 ml 0.1M $Na_4P_2O_7$ and 200 ml distilled water. The resulting mixture was dispersed in an ultrasonic bath for 10 minutes and shaken overnight. The clay fraction was freeze-dried and pre-mixed for XRD analysis. Detailed data of basalt and weathered basalt can be found in in Lei et al. (2025b).

2.4 Microscale analyses (Study II)

2.4.1 Sample preparation and optical microscopy measurements

Since both the P reference standards and microaggregates exhibit water stability, sample preparation involved suspending a small quantity (1-2 mg) of each powder in 10 mL of distilled

water (w/v), creating a homogeneous mixture through gentle agitation. A 20 µL aliquot of this suspension was then deposited onto a silicon (Si) wafer and allowed to air-dry at ambient temperature. The resulting fine particulate matter adhered to the wafer surface, forming a suitable substrate for subsequent optical imaging and NanoSIMS analysis. All specimens were mounted on silicon wafers and coated with a conductive layer of gold/palladium (Au/Pd) using a Polaron Emitech SC7640 sputter coater to mitigate charging effects during analysis.

An Axio Imager Z2 optical microscope (Zeiss) was employed to identify appropriate analysis regions, prioritizing flat-surfaced particles to minimize topographic artifacts and selecting exhibiting visible organo-mineral associations. For each soil type, 3 to 6 microaggregates were chosen, resulting in a total of 18 soil microaggregate observations. For the standards, three replicates per compound were measured due to their high homogeneity.

2.4.2 NanoSIMS measurements

NanoSIMS measurements were conducted using NanoSIMS 50L (Cameca, Gennevilliers, France) at the Technische Universität München. Both Cs^+ and O^- RF plasma sources (Malherbe et al., 2016) were employed for soil samples, while Cs^+ was used exclusively for the P standard compounds. Image acquisition was performed at a resolution of 256 x 256 pixels over a 30 µm x 30 µm field of view, with 40 sequential image planes captured. The dwell time was 1ms per pixel, the primary current 2pA for Cs^+ and 5pA for O^-. For Cs^+ source, the distribution of secondary ions including $^{16}O^-$, $^{12}C^-$, $^{12}C^{14}N^-$, $^{31}P^-$, $^{27}Al^{16}O^-$, $^{31}P^{16}O_2^-$, $^{56}Fe^{16}O^-$ were recorded. The $^{12}C^-$ and $^{12}C^{14}N^-$ channels were used to identify the distribution of OM and the two P-signals ($^{31}P^-$ and $^{31}PO_2^-$) were used to distinguish between OP and IP dominated regions. With the O^- source, ion detection included $^{23}Na^+$, $^{24}Mg^+$, $^{27}Al^+$, $^{28}Si^+$, $^{39}K^+$, $^{40}Ca^+$ and $^{56}Fe^+$ were used to provide detailed spatial resolution of mineral distributions.

2.5 Statistical analyses (Study I, II, III)

Across all studies, rigorous statistical analyses were performed in R (v4.3.1).

2.5.1 Study I

Linear mixed-effects model ('lme4' and 'lmerTest' packages) evaluated stocks of OC, TN, TP, OP and IP as functions of fixed effects (land use, depth, weathering index) and random effects (site, slope position, pseudo-replicates). Variance inflation factors (VIF < 5) screened for collinearity. Marginal (R^2m) and conditional (R^2c) pseudo-R^2 values ('margins' package) were reported.

Where land use effect was significant, two-way ANOVA ('car' package) compared contrast land uses on the slope and compared slope vs. flood plain ($\alpha = 0.05$). Homogeneity (Levene's

test) and normality (Shapiro-Wilk) were employed. Skewed data were log-transformed, with linear regression applied afterwords. Tukey's HSD provided post-hoc comparison. Stoichiometric relationships of C, N and P in bulk, fine and coarse fractions were assessed via linear and log regressions.

2.5.2 Study II

Secondary-ion images were drift- and dwell-time-corrected in Fiji (Open MIMS) and co-registered across Cs^+ and O^- sources. An unsupervised two-step clustering (Elbow-informed K-Means combined with hierarchical agglomeration and Ward linkage and Gap Statistic) on P- and mineral-element ion ratios yielded final clusters for OP, IP, six mineral/OM classes and background noise.

Relative abundances of P forms between land uses were compared with one-way ANOVA ($\alpha = 0.05$).

2.5.3 Study III

Two-way ANOVA ($\alpha = 0.05$) with Tukey's HSD assessed basalt treatment effects on TC, SOC, SIC, pH, eCEC, exchangeable Ca/Mg, and new/native C fluxes, validating assumptions with Levene's and Shapiro-Wilk tests.

PCA reduced predictor redundancy and identified covariation among soil physicochemical variables. A Random Forest model ('randomForest' and 'caret' packages) with k-fold cross-validation optimized m-try and evaluated out-of-bag error and RMSE. Variable importance rankings highlighted the strongest drivers of SOC and SIC contents.

3 Results

3.1 Results summary of Study I & III

In a South-east hillslope-flood plain system under comparable organic fertilization, long-term grassland and cropland diverged significantly in their organic carbon (OC) and total nitrogen (TN) stocks across the soil profile. Grassland soils exhibited higher OC and TN stocks in both the topsoil and subsoil, as evidenced by lower $\delta^{15}N$ signatures that signal reduced N losses compared to cropland soils. Although both land uses maintained similar total phosphorus (TP) stocks, cropland exhibited higher inorganic phosphorus (IP) stocks in the topsoil, likely reflecting fertilizer-derived inputs, offset by depleted organic phosphorus (OP) stocks in the subsoil due to less organic matter (OM) inputs caused by clear-harvest practices and soil degradation. In contrast, grassland showed a higher OP stock in the subsoil.

Particle size fractionation revealed that both OC and OP concentrate in the fine-silt and clay sized (<20 μm) fraction regardless of land use and soil development processes, but the fine fraction of grassland soils showed a higher OP:TP ratio. In addition, stoichiometric correlation of OC:OP in the fine fraction (20:1 - 60:1) was close to microbial C:P ratios (23:1 - 100:1), pointing to a biotic driven pathway (immobilization/assimilation of OP in microbial biomass/necromass) playing a critical role in grassland P retention, whereas narrower OC:OP ratios under cropland (25:1 - 35:1) implied the dominant of direct association of P with mineral surfaces.

Fresh basalt increased soil pH significantly due to its enrichment in olivine, that can rapidly neutralize H^+, release Mg^{2+} and foster bicarbonate alkalinity. These combined effects enhanced the dissolved inorganic carbon (DIC) formation and boosted soil inorganic carbon (SIC) stocks by ~4% over six months, but at the cost of a substantial (~17%) loss of soil organic carbon (SOC). As olivine depleted through weathering, ground-weathered basalt shifts to Ca^{2+} dominated dissolution, maintained SIC gains (~4%) without altering pH, and curtailed SOC losses comparable to the control soils (~7%). Ground-weathered basalt, with its high specific surface area and Ca-mediated organo-mineral associations, enhanced retention of both native and added (straw-derived) OC, pointing to its two roles in soil acidity correction and enhanced OC stabilization. When plant residues were present, the free H^+ released by residue decomposition partially suppressed DIC formation, reducing SIC and effluent DIC accrual relative to those without new residue inputs.

3.1.1 Bulk soil OC, TN, TP, OP, IP contents, and $\delta^{15}N$ signature (Study I)

Grassland use had higher OC, TN and OP stocks in the topsoil (0 - 20 cm) than cropland on the slope. In grassland, these stocks fell sharply with depth, from 65 mg OC g^{-1}, 4.7 mg TN g^{-1}

and 0.79 mg OP g^{-1} at 0-5 cm to 13 mg OC g^{-1}, 1.3 mg TN g^{-1} and 0.43 mg OP g^{-1} at 15 - 20 cm. Cropland soils, by contrast, had uniform values (16 mg OC g^{-1}, 1.6 mg TN g^{-1}, 0.45 mg OP g^{-1}) through the top 20 cm, then declined sharply below 40 cm where the BC horizon started.

The $\delta^{15}N$ in cropland topsoil stayed constant at 6 - 7 ‰, whereas grassland started lower (3 - 4.5 ‰) in the topsoil and converged with cropland by 10 - 20 cm. Grassland topsoil was OP-rich, with OP making up over 50 % of TP (mean ≈ 67 %), while cropland was IP-dominated (<50 % OP in the Ap horizon, ≤20 % in subsoil). Inorganic P remained stable with depth across both land uses on the slope. Statistical tests confirmed significant land use effects on OC, TN, TP and OP along the slope.

Flood plain soils showed no OC or TN content differences in either topsoil or subsoil. Only IP content was higher in Phaeozem, and TP in both soil profiles was dominated by inorganic form.

3.1.2 Bulk soil OC, TN, TP, OP and IP stocks (Study I)

A linear mixed model was used to separate land use effects on stocks from site variability. Random effects explained up to ~40 % of the variance, but after accounting for them, only OC stocks differed significantly with land use throughout both depth intervals (0 - 20 cm and 0 - 60 cm).

On the slope, grassland had higher OC stocks in the topsoil (40 Mg ha^{-1}) than cropland (30 Mg ha^{-1}) but had lower IP stocks. Taking the subsoil into account (20 - 60 cm), grassland also surpassed cropland in TN and OP stocks, with mean stocks of 71 Mg OC, 6.5 Mg TN and 2.2 Mg OP ha^{-1} versus 50, 4.7 and 1.7 Mg ha^{-1}, respectively. In both land uses on the slope, OC and TN stocks were concentrated in the first 20 cm.

Cropland topsoil was dominated by IP, where OP made up only 39 - 4 % of TP stocks. Grassland, in contrast, showed a rising OP share downslope, from 46% on the upper part to 58% on the lower part of the slope. In the subsoil, IP dominated TP stocks regardless of land uses.

Comparing landscape positions, slope and flood plain topsoils did not differ in OC, TN and TP stocks. When the whole soil profile was considered, however, the flood plain contained higher OC, TN, TP and IP stocks, while OP stocks stayed comparable between the two.

3.1.3 Molecular components of bulk soil derived from solid-state ^{13}C NMR spectroscopy (Study I)

Solid-state ^{13}C NMR spectroscopy of A horizon of soil profiles revealed that grassland contained more O-alkyl-C and exhibited lower alkyl/O-alkyl-C ratios than their cropland

counterparts. In both land uses, alkyl:O-alkyl-C ratio tended to decline downslope. Molecular mixing model showed that grassland A horizons were richer in carbohydrates (≈ 34 %) and poorer in lignin, whereas all soils contained only 3 - 6% char.

On the slope, alkyl/O-alkyl-C ratio in the fine fraction correlated linearly with both OC:OP and OC:TN ratios. In the flood plain, it correlated only with OC:OP ratio. Higher OC:OP ratio and OC:TN ratio were associated with narrower alkyl:O-alkyl-C ratios

3.1.4 The distribution and enrichment of OC and OP in the fine and coarse fractions (Study I)

The distribution of OC and OP pools in different soil fractions was shown in Figure 3. Within the A horizons of the soil profiles, the fine fractions for both land uses on the slope were dominated by OC and OP, ranging from 70 % to 83 % for OC and 84 % to 93 % for OP, with OP always more concentrated than OC. The proportion of OP in the fine fraction was higher than that of OC. The OP/TP proportion was higher on the slope than on the flood plain. Enrichment factors with values exceeding 1 for OC, TN and OP in the fine fraction confirmed their dominance in the fine fraction.

Within the fine fraction, OP dominated the TP pool and showed significantly higher abundance in grassland than cropland. The coarse fraction was largely IP-dominated, with OP contributing <10 % and showing no land use effect.

Soils on the slope showed positive correlations among OC, TN and OP contents in the fine fraction, while in the flood plain, only OC and TN contents were correlated, with OP behaving independently.

3.1.5 OC:TN ratio to OC:OP ratio and their correlation with OC in bulk soils, fine and coarse soil fractions (Study I)

The OC:OP ratio declined rapidly in the top 10 cm of grassland on the slope, then settled near 30:1 through the rest of the soil profile. Flood plain soils followed the same changing pattern with higher ratio (50:1), whereas cropland stayed at approximately 30:1 in the A horizon with continuous decline in the B horizon. In the fine fraction, OC:TN ratio ranged from 9 to 13 and OC:OP ratio ranged from 19 to 61. The coarse fractions had much higher OC:OP ratios, ranging from 90 to 550.

Stoichiometric coupling varied by context. Bulk soil and fine fractions in cropland showed no correlation between OC:TN and OC:OP ratios, while grassland on the slope exhibited a positive relationship between the two ratios. The coarse fraction was the opposite in cropland on the slope and in the flood plain, with a higher OC:OP ratio corresponding to a higher OC:TN ratio.

Log-regressions of natural log-transformed OC:TN and OC:OP ratios against OC content indicated both ratios rise with increasing OC until a plateau at ≈ 85 mg OC g^{-1}, beyond which OC:TN ratio stayed < 12:1 and OC:OP < 90:1. Across the slope, OC:TN ratios consistently exceeded 12 and OC:OP exceeded 72 irrespective of land uses.

3.1.6 Soil C contents, $\delta^{13}C$ analysis and physicochemical properties after 6-months of incubation (Study III)

After 6 months of incubation, total C (TC) content declined in all treatments. The most significant decline occurred in fresh basalt treatments, whereas weathered and ground weathered basalt were similar to the control soils. When straw was added, TC content dropped the most in the weathered basalt treatments yet still did not differ from the straw-only control soils. All straw treatments maintained higher TC content than the soils without straw.

The SOC content of fresh and weathered basalt ended up 10 % and 8 % below the control soils, respectively, while ground weathered basalt had a marginal change compared to the control soils. In soils without additional straw added, all basalt treatments promoted soil inorganic carbon (SIC) accumulation, whereas the presence of straw limited those SIC differences as there was none SIC accrual observed.

After 6-months incubation, over 75% of straw-derived OC had been mineralized across all treatments. Soils receiving ground weathered basalt retained the most straw-derived OC, exceeding the control soils, while fresh basalt retained the least straw-derived OC.

Fresh basalt increased soil pH, effective CEC (eCEC) and exchangeable Mg^{2+} content relative to the control soils, with exchangeable Ca^{2+} unchanged. Weathered and ground weathered basalt, with or without straw, showed a marginal pH alternation but had a higher exchangeable Ca^{2+} content.

After 6 months of incubation, particle size distribution remained unchanged across all treatments. Specific surface area (SSA) was unaltered by fresh basalt but rose to ~10 m^2 g^{-1} in soils treated with weathered or ground weathered basalt.

3.1.7 Random Forest model for explaining SOC and SIC contents (Study III)

The PCA analysis showed that soil pH, eCEC, SSA and the exchangeable Ca^{2+} and Mg^{2+} were the primary factors determining SOC and SIC contents. Within these five variables, Random Forest model accounted for > 75 % of SOC variance and > 55 % of SIC variance, with RMSE values below 0.20. For SOC, eCEC, exchangeable Mg^{2+} and pH were the strongest predictors; while for SIC, the best explanatory variable was SOC, exchangeable Mg^{2+} and Ca^{2+}. Model

predicted outputs fit the measurement values closely, with adjusted R^2 of roughly 0.95 for SOC and 0.91 for SIC.

3.1.8 The C balance and fluxes in the atmosphere-soil-effluent system (Study III)

The C recoveries of all treatments, except for the weathered basalt was over 90%. Fresh basalt increased effluent pH as well as DOC, DIC and dissolved Mg content in the effluent. Ground weathered basalt showed limited DOC content increasing with lower concentration of dissolved Mg and Ca. After 6 months, fresh basalt shifted the leachate from DOC- to DIC-dominance, whereas weathered and ground-weathered basalt had DIC content unchanged.

Fresh basalt increased the IC pool gain (SIC + DIC) to ~4 % of C within the system, which was four times higher than the control soils. However, it also led to significant amounts of SOC losses. Net C losses (SOC loss + IC gain) were ~6 % for the control soils, 13 % for fresh basalt treatments, 10 % for weathered basalt treatments and 6 % for ground weathered basalt treatments (Table 1).

Straw addition promoted CO_2 release to 10 - 11 % of C and suppressed SIC accumulation, with SIC content declining from 3 - 4 % to < 1 % in all basalt treatments. Effluent DIC content remained at a very low level (<1 %). Ground weathered basalt combined with straw maintained SOC levels comparable to the straw-only control soils.

3.2 Results summary of the unpublished Study II

Based on the bulk analyses information from Study I, unpublished Study II went further to understand the OP and IP spatial distribution on microaggregate surfaces. Combining NanoSIMS measurements with unsupervised two-step segmentation based on P and N related ratios ($^{31}P^{16}O_2^-/(^{31}P^- + {}^{31}P^{16}O_2^-)$ and $^{12}C^{14}N^-/(^{12}C^- + {}^{12}C^{14}N^-)$), this study differentiated soil microaggregate surface regions into four distinct P-compound clusters, which were *myo*-inositol hexaphosphate dominated, aluminum/iron phosphate dominated, microbial biomass dominated and N-rich OP compounds characterized by low $^{31}P^{16}O_2^-$ ratios coupled with elevated N signals indicative of amino- or nucleotide-based OP compounds. Four temperate soils (Cambisol, Luvisol, Phaeozem, Fluvisol) of comparable mineral composition but divergent bulk OC, P partitioning and P availability were used. Subsequently, P distributions relative to six mineral/organic classes (‘Phyllosilicates’, ‘MAOM’, ‘OM’, ‘Other Si-minerals’, ‘Ca oxides’, ‘Quartz’) were mapped on microaggregate surfaces. Across all soils, over 85% of P hotspots occurred on OM-free phyllosilicate surfaces and their associated OM coatings (53% on bare phyllosilicate, 34% on phyllosilicate-MAOM), whereas Fe/Al (hydr)oxides were virtually absent (<0.5 % by mass) and contributed negligibly to total P retention. In the fine fraction of the low-OC Cambisol (OP ≈ IP), IP-mineral complexes dominated microaggregate surfaces. By

contrast, the high-OC Luvisol (≈ 82% OP) exhibited extensive coverage by N-rich OP compounds and microbial biomass dominated compounds. These contrasting spatial patterns thereby confirmed the two P retention pathways from Study I: an N-independent retention pathway, in which IP and N-poor OP sorbed to OM-free mineral surfaces determined P release kinetics, and an N-rich pathway, in which OM associated P were solubilized and went through enzymatic cleavage by microbial communities. The decoupling of N and P cycling, evidenced by weak bulk N:P correlations from Study I in these soils, was thus a function of the relative dominance of either pathway.

In this study, I am responsible for soil sampling pretreatment and preparation for NanoSIMS measurements, including all soil physicochemical analyses and related data processing. I am the primary contributor for conceptualization, data analysis and manuscript draft.

4 Discussion

4.1 Distinct effect of land use and soil development processes on carbon, nitrogen and phosphorus cycling in the flood plain and hillslope in temperate zones

On the hillslope, where soils have developed under comparable pedogenic conditions and have undergone similar organic fertilization regimes for three decades, grassland soils demonstrate significantly higher organic carbon (OC) stocks in both the topsoil (0 - 20 cm) and the subsoil (20 - 60 cm) than adjacent cropland soils (Fig. 4.1a, b; Study I). This discrepancy is attributed to increased organic matter (OM) inputs, more rapid root turnover, and the preservation of a well-developed B horizon. In contrast, cropland soils exhibit lower OC stocks due to lower OM input from clear-harvest practices supported by elevated alkyl/O-alkyl-C ratios (Table 4.1; Study I), and soil structure degradation indicated by a lower OC:Clay ratio (Prout et al., 2021) (Study I). The presence of BC horizons following the Ap horizon (Chaplot and Poesen, 2012; Van Oost et al., 2007), along with a high soil bulk density, indicate the occurrence of soil erosion. Total nitrogen (TN) stocks show significant differences only in the subsoil, with grassland subsoils retaining more TN than cropland subsoils due to the well-preserved B horizon. TN stocks do not differ substantially in the topsoil between the two land uses on the slope (Study I). The higher TN stocks in grassland soils are aligned with isotopic evidence from the $\delta^{15}N$ signature, suggesting reduced N loss via gaseous pathways in grassland soils.

Phosphorus (P) stocks are shaped differently from OC and TN stocks, as the sources and cycling of P pools differ from OC and TN pools (Condron et al., 2005). Organic phosphorus (OP) is primarily linked to microbial-driven soil organic matter (SOM) decomposition, while inorganic phosphorus (IP) originates largely from the parent material with less contributions from SOM turnover by microbial processes (Gocke et al., 2021). On the hillslope, a higher SOM content in grassland soils supports a higher OP content in the topsoil, and a well-preserved B horizon rich in SOM further contributes to higher OP stocks in deeper horizons (Study I). The OP stock in cropland topsoil is not significantly lower due to its greater bulk density, which compensates for its lower OP content (Study I). The same parent material and comparable degree of mineral weathering, as indicated by similar Chemical Weathering Index (CWI) values, lead to consistent IP content between the two land uses (Study I). However, due to the higher bulk density and less SOM in cropland topsoil, IP stocks are predominant, consistent with patterns observed in other cropland soils (Cade-Menun, 2017; Stutter et al., 2015; Von Sperber et al., 2017). Thus, while OP stocks are lower in cropland subsoils, the higher IP stocks in the topsoil result in comparable total phosphorus (TP) stocks between the two land uses (Fig. 4.1c; Study I), with the dominance of IP stocks, particularly in the subsoil (Study I).

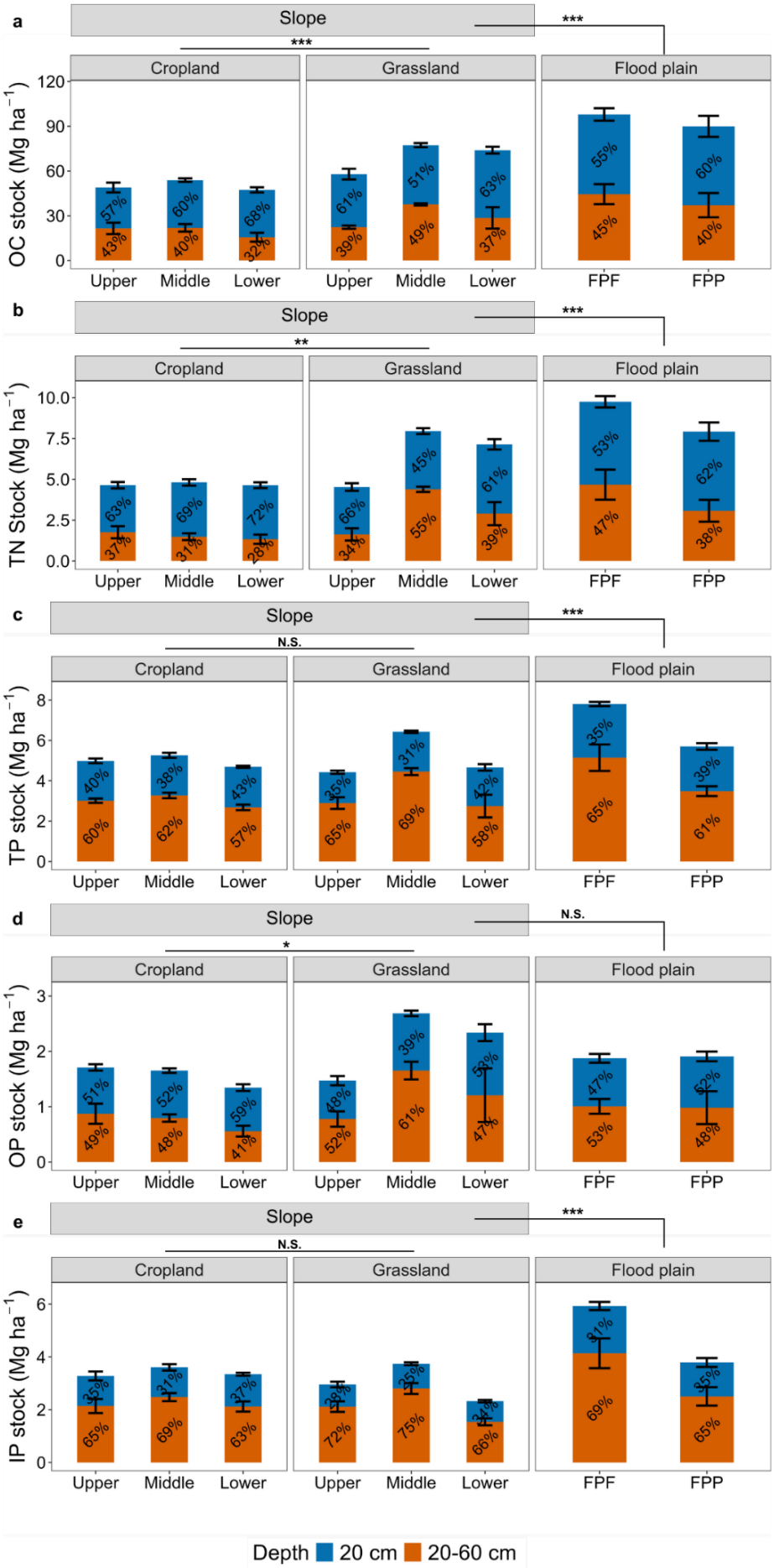
a
Slope
***
***
Cropland
Grassland
Flood plain
OC stock (Mg ha^{-1})
120
90
60
30
0
57%
43%
60%
40%
68%
32%
61%
39%
51%
49%
63%
37%
55%
45%
60%
40%
Upper
Middle
Lower
Upper
Middle
Lower
FPF
FPP
b
Slope
***
**
Cropland
Grassland
Flood plain
TN Stock (Mg ha^{-1})
10.0
7.5
5.0
2.5
0.0
63%
37%
69%
31%
72%
28%
66%
34%
45%
55%
61%
39%
53%
47%
62%
38%
Upper
Middle
Lower
Upper
Middle
Lower
FPF
FPP
c
Slope
***
N.S.
Cropland
Grassland
Flood plain
TP stock (Mg ha^{-1})
8
6
4
2
0
40%
60%
38%
62%
43%
57%
35%
65%
31%
69%
42%
58%
35%
65%
39%
61%
Upper
Middle
Lower
Upper
Middle
Lower
FPF
FPP
d
Slope
N.S.
*
Cropland
Grassland
Flood plain
OP stock (Mg ha^{-1})
3
2
1
0
51%
49%
52%
48%
59%
41%
48%
52%
39%
61%
58%
47%
47%
53%
52%
48%
Upper
Middle
Lower
Upper
Middle
Lower
FPF
FPP
e
Slope
***
N.S.
Cropland
Grassland
Flood plain
IP stock (Mg ha^{-1})
6
4
2
0
35%
65%
31%
69%
37%
63%
28%
72%
25%
75%
34%
66%
31%
69%
35%
65%
Upper
Middle
Lower
Upper
Middle
Lower
FPF
FPP
Depth
20 cm
20-60 cm

Fig. 4.1 The stocks of **(a)** organic carbon (OC), **(b)** total nitrogen (TN), **(c)** total phosphorus (TP), **(d)** organic phosphorus (OP) and **(e)** inorganic phosphorus (IP) in grassland and cropland soils on the hillslope and flood plain. Their respective stocks in the topsoil and subsoil are marked as blue and orange color. Data are mean ± SE, n = 4. The 'Upper', 'Middle', and 'Lower' mean the upper, middle, and lower parts of the slope. The asterisk in 'Cropland' and 'Grassland' means the significant level of 0 - 60 cm stocks between land uses on the slope, and the asterisk in 'Flood plain' means the significant level of 0 - 60 cm stocks between the slope and flood plain from ANOVA. The asterisk ('*') indicates $0.01 < p < 0.05$, '**' indicates $0.001 < p < 0.01$, '***' indicates $p < 0.001$. The non-significant comparison is marked as '*N.S.*'. (Figure is taken from Study I).

The flood plain under extensive grassland use shows significantly higher OC, TN, TP, and IP stocks across the entire soil profile compared to the hillslope (Fig. 4.1; Study I). These differences are primarily attributed to different soil development processes, where the flood plain subsoil is developed through long-term colluvial and alluvial sedimentation and is influenced by groundwater besides its granite origin. The presence of thick Cl/Cr horizons and evidence from historical maps (Fig. 2.1; Study I) corroborate these depositional processes. Accumulation of OM through flooding and sediment inputs (Martínez-Mena et al., 2019; Mayer et al., 2018) leads to significantly higher OC and TN stocks. In addition, the subsoil exhibits higher IP stocks, likely due to P inputs via groundwater and subsequent sorption processes (Weihrauch and Weber, 2021), resulting in higher TP stocks in the flood plain than on the hillslope (Study I). No significant differences in OC, TN, or TP are observed in the top A horizon, where land use is the dominant determining factor, as evidenced by the presence of the Ah horizon (Fig. 2.1; Study I).

The OC, TN, and P stocks provide an overall map of their distribution and abundance in the topsoil and subsoil, reflecting the distinct impacts of land use and soil development processes on their stocks. This prompts interest in factors controlling their availability and stabilization, especially P, which are also essential for long-term sustainable P use in the face of mineral-P depletion and soil degradation.

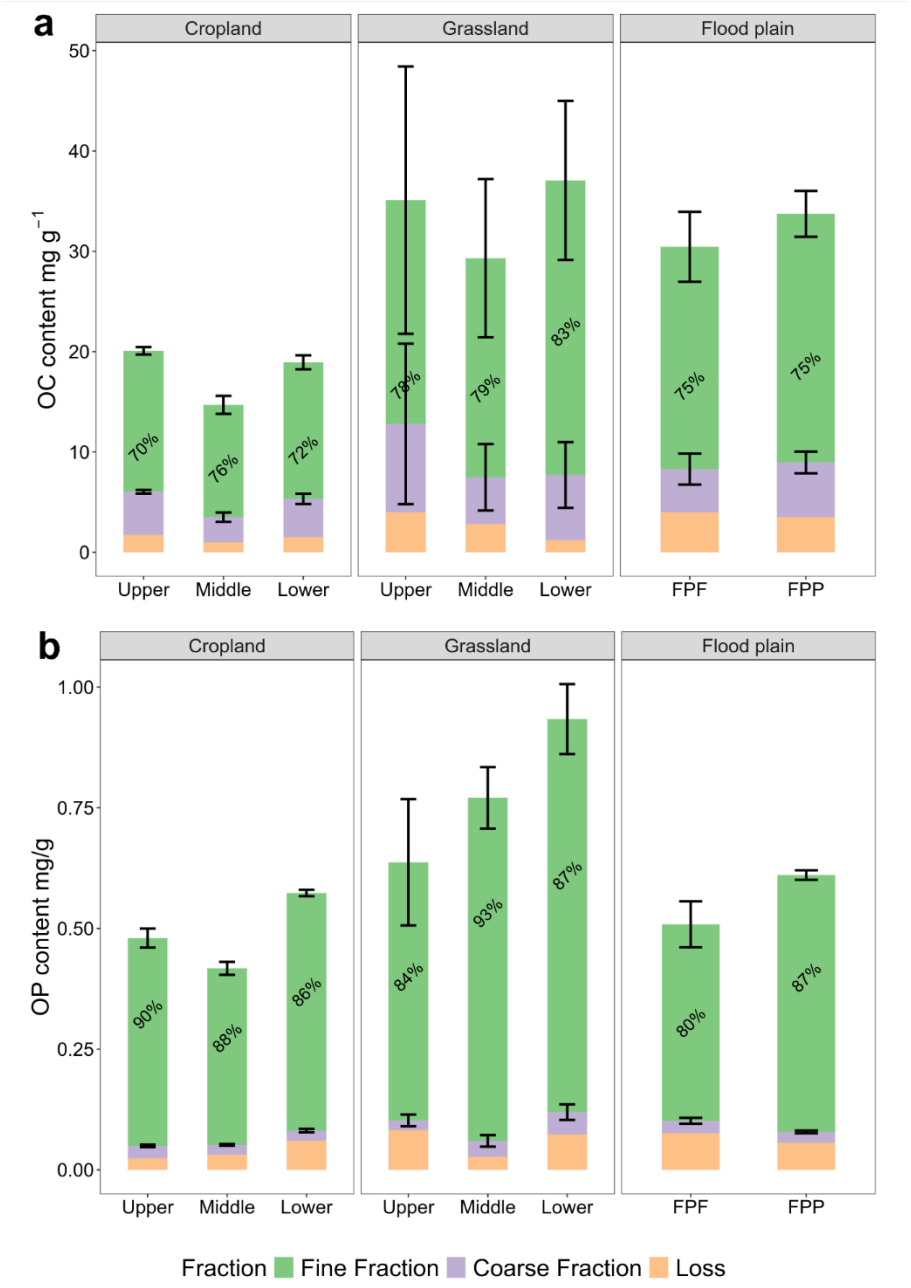

Fig. 4.2 The **(a)** OC content and **(b)** OP content in the A horizon of each soil profile depict for cropland and grassland on the slope and flood plain. Samples are collected at different depths in the A horizon. Data are the mean value of each depth in the A horizon ± SE. The loss fractions are presented as mean values only. 'Upper', 'Middle', 'Lower', 'FPF', and 'FPP' means the upper, middle, and lower parts of the slope, Fluvisol, and Phaeozem in the flood plain, respectively. (Figure is taken from Study I).

By soil particle size fractionation, topsoils were fractionated into fine (<20 µm) and coarse (>20 µm) fractions (Just et al., 2021), representing fractions rich in particulate organic matter (POM) and mineral associated organic matter (MAOM), respectively. In all soils, regardless of land uses and soil development processes, OC, TN, and OP are concentrated in the fine fraction, consistent with findings across various climatic zones (Spohn, 2020b), while IP is more abundant in the coarse fraction (Fig. 4.2; Study I). Over 70% of OC and 85% of OP are found

in the fine fraction, with an enrichment factor >1 (Table 4.1; Study I), confirming their preferential stabilization in the fine fraction. This general pattern of OC and OP distribution across particle-size fractions remains unaffected by land uses or soil development processes. However, land use significantly affects the OP/TP proportion, specifically in the fine fraction. Grassland soils have consistently higher OP enrichment than cropland soils (Table 4.1; Study I), aligning with higher OP content in bulk topsoils. This suggests that the land use-driven OP content alteration in the topsoil may primarily be associated with OP allocation in the fine fraction.

Table 4.1 The OC:TN:OP stoichiometry in the fine and coarse fraction of the A horizon in soils. The enrichment factor is calculated by the OC/TN/OP content in each fraction divided by the OC/TN/OP content in bulk soil. Data are the mean of each depth in the A horizon ± SE. 'Upper', 'Middle', 'Lower', 'FPF', and 'FPP' means the upper, middle, and lower parts of the slope, Fluvisol, and Phaeozem in the flood plain, respectively. (Table is taken and modified from Study I).

Location	Part	Fraction	OC:TN	OC:OP	OP/TP	OC Enrichment Factor	TN Enrichment Factor	OP Enrichment Factor
/	/	/	/	/	%	/	/	/
Grassland on the slope	Upper	Fine	10 ± 1.0	35 ± 13	66 ± 8	1.9 ± 0.40	2.0 ± 0.39	2.0 ± 0.21
		Coarse	32 ± 7.1	251 ± 151	4.5 ± 0.37	0.30 ± 0.17	0.17 ± 0.13	0.05 ± 0.03
	Middle	Fine	11 ± 0.5	30 ± 8.4	75 ± 1.0	1.7 ± 0.22	1.8 ± 0.34	1.9 ± 0.07
		Coarse	19 ± 2.6	120 ± 57	7.4 ± 2.7	0.28 ± 0.11	0.17 ± 0.05	0.08 ± 0.02
	Lower	Fine	10 ± 0	35 ± 6.5	86 ± 2.0	1.7 ± 0.18	1.8 ± 0.18	1.8 ± 0.05
		Coarse	17 ± 0.62	126 ± 23	13 ± 4.2	0.34 ± 0.10	0.22 ± 0.08	0.11 ± 0.04
Cropland on the slope	Upper	Fine	10 ± 0	33 ± 0.9	54 ± 1.5	1.3 ± 0.04	1.5 ± 0.14	1.7 ± 0.03
		Coarse	20 ± 0.32	172 ± 16	7.8 ± 0.50	0.47 ± 0.03	0.26 ± 0.02	0.12 ± 0.01
	Middle	Fine	10 ± 0	30 ± 1.5	50 ± 0.42	1.5 ± 0.02	1.5 ± 0.15	1.7 ± 0.04
		Coarse	16 ± 0.51	119 ± 12	6.8 ± 0.64	0.36 ± 0.05	0.22 ± 0.03	0.11 ± 0.01
	Lower	Fine	10 ± 0	28 ± 1.6	59 ± 0.74	1.5 ± 0.01	1.4 ± 0.06	1.8 ± 0.07
		Coarse	18 ± 0.28	167 ± 19	6.0 ± 0.90	0.41 ± 0.02	0.22 ± 0.03	0.08 ± 0.01
Flood plain	FPF	Fine	10 ± 0	54 ± 2.7	53 ± 3.7	1.5 ± 0.13	1.6 ± 0.09	1.6 ± 0.09
		Coarse	18 ± 0.91	157 ± 27	6.5 ± 1.9	0.30 ± 0.07	0.17 ± 0.04	0.11 ± 0.02
	FPP	Fine	11 ± 0.5	46 ± 3.5	65 ± 2.0	1.6 ± 0.12	1.6 ± 0.06	1.8 ± 0.04
		Coarse	20 ± 0.53	241 ± 20	5.2 ± 0.60	0.31 ± 0.02	0.17 ± 0.02	0.07 ± 0.01

In summary, land use and soil development processes have distinct yet interacting impacts on the vertical and particle distribution of OC, TN and different forms of P. Under comparable soil development processes (e.g., hillslope in Study I), grassland soils can retain significantly higher stocks of OC, TN and OP compared to cropland soils, primarily attributing to continuous above- and below-ground biomass inputs and well-preserved B horizons, whereas cropland soils exhibit significant lower OC and TN stocks due to soil structural degradation and erosion.

Flood plain soils are decoupled from the hillslope soils with respect to the C-N-P stocks due to their different soil development processes, with flood plain subsoils largely impacted by colluvial and alluvial sedimentation and groundwater besides its granite origin, while the topsoil is highly determined by land use. Regardless of land use and soil development processes, OC, TN and OP pools are enriched in the fine fraction (mainly consisting of MAOM), while the IP pool is concentrated in the coarse fraction (mainly consisting of POM). These quantity and quality assessments of C-N-P emphasize that the coupled degree between OC, TN and P pools can be primarily impacted by land uses and soil development processes, particularly considering different P forms. OP and IP partitioning and distribution can be highly dependent on land uses, thereby emphasizing the importance of proper management for sustainable P utilization.

4.2 The two potential pathways for phosphorus retention and availability associated with organic carbon and nitrogen cycling

The biogeochemical cycles of OC, N, and P are generally regarded as tightly coupled, meaning that soils with high OC stocks also typically store significant amounts of N and P stocks (Spohn, 2020a), and vice versa. Although plant- and microbe-derived OM can span a wide range of C:N ratios, the MAOM fraction in soils remains a constant C:N ratio of ~ 12:1 (Cotrufo et al., 2019). Some studies attribute this consistency to the inherent stoichiometry of recalcitrant OM, whereas some claim it to microbial immobilization, where the C is assimilated into microbial biomass/necromass and subsequently stabilized onto mineral surfaces or occluded within soil aggregates (Kögel-Knabner et al., 2008). This results in using OC:TN ratio as a qualitative indicator of SOM stabilization and composition. A narrow OC:TN ratio thereby can suggest active microbial decomposing and well-immobilization of plant-derived OC into microbial biomass/necromass (Cotrufo et al., 2019; Kögel-Knabner et al., 2008), leading to an N-enriched MAOM fraction with an OC:TN ratio close to that of microbial biomass C:N (Cotrufo et al., 2019). Moreover, given the parallel enrichment of OC and OP in fine fractions, Spohn (Spohn, 2020a, b) suggests that OP may follow similar stabilization pathways as OC in soils, implying a significant OP immobilization/assimilation within microbial biomass/necromass and subsequent association with mineral surfaces.

The OC:TN ratio observed in the fine fraction of these soil ranges from 9:1 to 11:1 (Fig. 4.3a; Study I), which is within the stoichiometric ratio that suggests a high proportion of OC stabilized in microbial biomass/necromass (Cotrufo et al., 2019; Kögel-Knabner et al., 2008). Combined with the fact that the OC and OP show a comparable enrichment (>1) in the fine fraction, with an OC:OP ratio ranging from 20:1 to 60:1 (Fig. 4.3a; Study I) that aligns with microbial biomass C:P ratios (23:1 ~ 100:1, average approximately 60:1) in grassland and arable soils (Cleveland

and Liptzin, 2007; Griffiths et al., 2012; Heuck et al., 2015; Khan and Joergensen, 2019; Turner et al., 2013; Xu et al., 2013), these two evidence suggest that a considerable portion of OP may be immobilized/assimilated in microbial biomass/necromass alongside OC through organo-mineral associations, correlating with organic N.

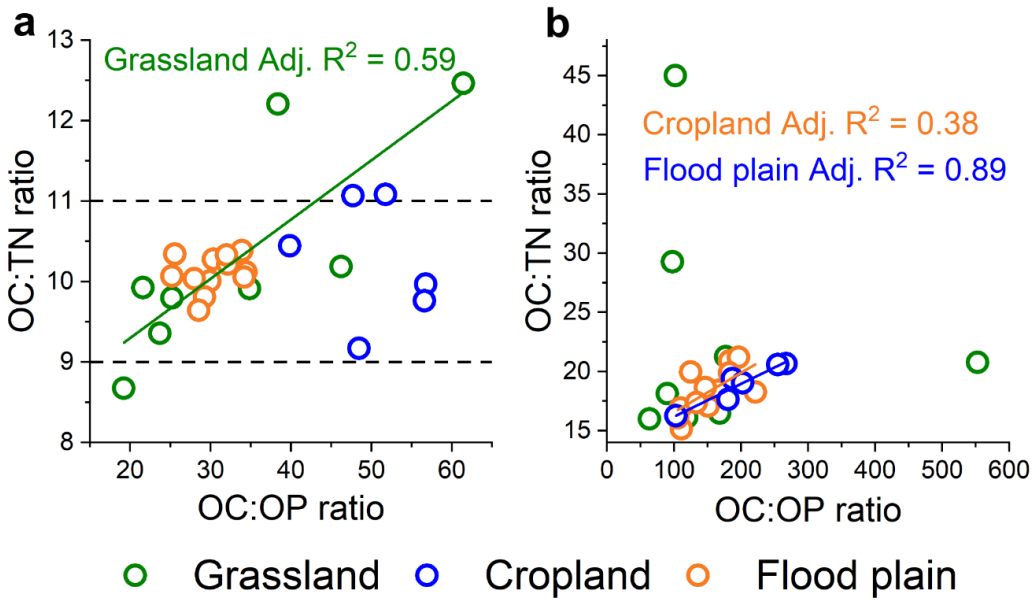

Fig. 4.3 (a) OC:TN ratio to OC:OP ratio in the fine fraction of the A horizon in the soil profile, **(b)** OC:TN ratio to OC:OP ratio in the coarse fraction of A horizon in the soil profile. (Figure is taken and modified from Study I)

At the same time, this work observes that OP correlations with TN are weaker than the correlation between OC and TN (Study I), as also noted by Williams and Steinbergs (1959). Combined with a narrower OC:OP ratio than the microbial biomass C:P, along with lower $\delta^{15}N$ values in some grassland topsoils, this may indicate the presence of an alternative OP stabilization pathway. This abiotic pathway may involve the sorption of N-independent OP compounds, such as mono/diester orthophosphates (e.g., inositol phosphates with C:P ratios of 1:1 to 11:1) (Condron et al., 2005), directly onto mineral surfaces. These forms are structurally resistant to enzymatic breakdown and can chelate to mineral surfaces due to the existence of several phosphate groups, particularly in clay-rich fine fractions (Condron et al., 2005; Spohn, 2024). This can be further supported by the limited accumulation of carbohydrates found in these soils associated with a higher alkyl:O-alkyl-C ratio (Study I) as carbohydrates mainly exist in less decomposed OM easily-available for microorganisms.

Further NanoSIMS measurements of these two soils confirm these hypotheses (Study II). By using four representative P reference standards with unsupervised segmentation, the hotspots of both OP and IP associated with different minerals and OM are identified and located. In NanoSIMS measurements, the immobilization of both OP and IP in OM and microorganisms

is observed in microaggregate surfaces, as well as those IP and OP compounds directly associated with OM-free mineral surfaces. Specifically, in the fine fraction of cropland soils, with an equal share of OP and IP (Study I), microaggregate surfaces are dominated by IP-dominated compounds (Fig. 4.4a; Study II). In contrast, with OP constituting ~ 82% of TP (Study I), microaggregate surfaces are enriched in OP-dominated compounds in the fine fraction of grassland soils, including those N-rich OP dominated compounds and microbial biomass/necromass (N-rich) (Fig. 4.4b; Study II).

In regions where OM is absent, and mineral surfaces are devoid of organic N (N-free, or with limited N fixed in mineral matrix), phosphorus is predominantly retained in the form of IP, or as N-poor OP compounds like *myo*-inositol hexaphosphate and glucose 6-phosphate. These regions represent an N-independent P retention pathway as was suspected from bulk analyses in Study I. In these regions, without the significant effect of microbial-induced biological processes, the P availability may be largely governed by its molecular structure and the sorption strength of P-mineral associations. Conversely, in regions with organic N involved, those N-rich OP compounds, including those concentrated in microbial biomass/necromass like nucleic acids, phosphatidylcholine, and teichoic acid (which often features D-alanine side chains), and N-containing compounds like adenosine di/triphosphate and 2-aminoethyl phosphonic acid, represent the N-rich P retention pathway (Fig. 4.4; Study II). These parts of P stored in OM show limited solubility without microbial processes due to the formation of stable ligand exchange between P and OM, which often requires the N-dependent microbial processes to release available P.

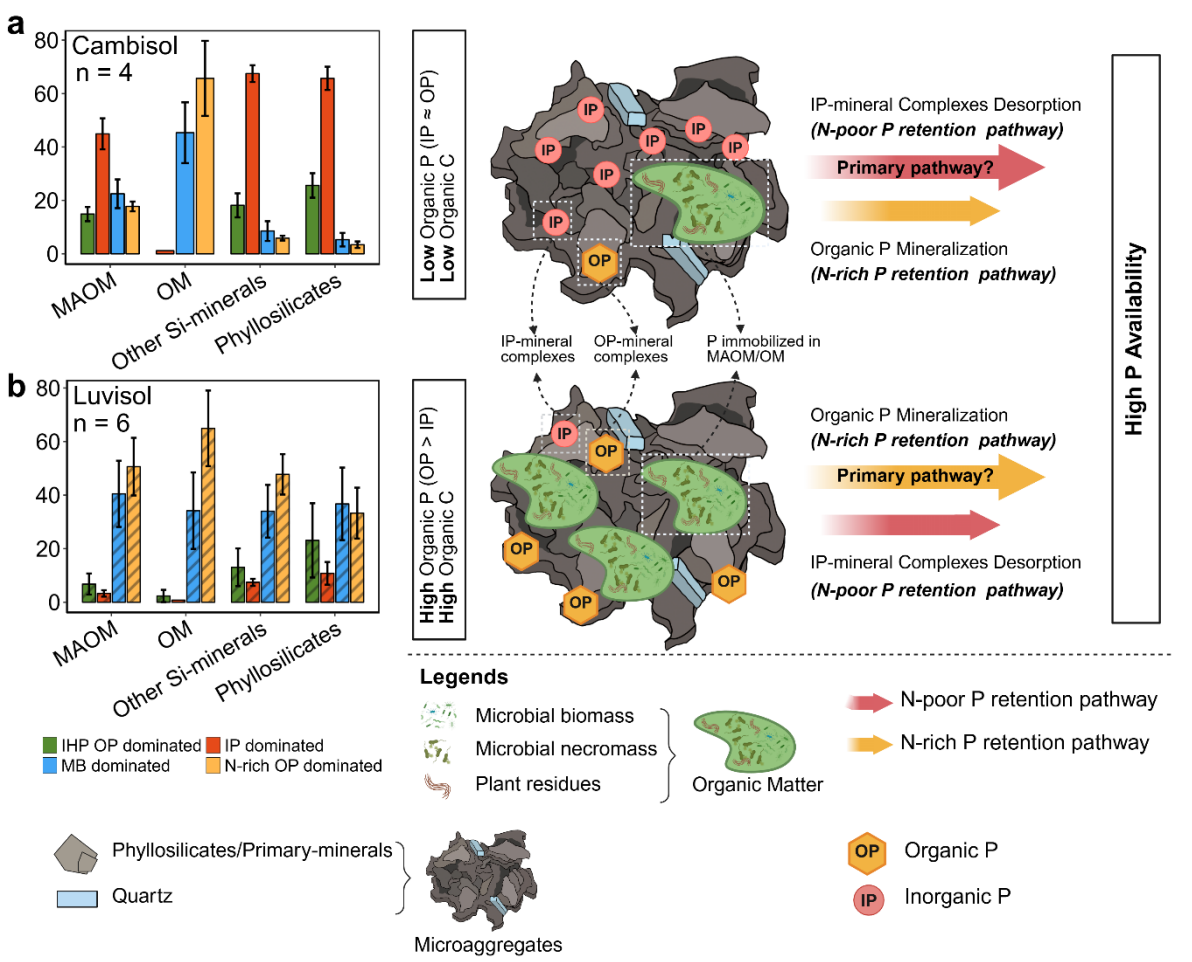

Fig. 4.4 The relative distribution and abundance of defined phosphorus (P) compounds on microaggregate surfaces from Cambisol and Luvisol, and their respective dominant P retention pathways related to co-occurrence of organic nitrogen (N). **(a)** Cropland (Cambisol) and **(b)** grassland (Luvisol). The 'No/Low P' regions are excluded in calculation. Data are mean ± SE, n = 4 for cropland (Cambisol) soils, n = 6 for grassland (Luvisol) soils. The 'IHP', 'IP' and 'MB' indicate *myo*-inositol hexaphosphate, $AlPO_4$ and $FePO_4$, and microbial biomass (derived from *Bacillus Subtilis*), respectively. (Figure is taken and modified from Study II)

Moreover, as the availability of P is concentrated in the fine fraction (mainly in microaggregates) and the available-P/TP proportion between the two land uses are similar (Study II), these two retention pathways thereby can also provide direct evidence that a high P availability does not necessitate IP pool dominance in soils. Instead, the dominance of OP pool can equally achieve high P availability with a high level of OC and organic N pools observed in grassland.

In the fine fraction of cropland soils, microaggregate surfaces are predominantly covered by IP-mineral complexes, particularly IP-phyllosilicates complexes (Fig. 4.4; Study II). Numerous sorption-desorption experiments (Amadou et al., 2022; Bollyn et al., 2017; Celi et al., 2003; Martin et al., 2004) have consistently shown that IP-mineral complexes generally have weaker adsorption strength due to the formation of outer-sphere complexes through electrostatic

forces that are more easily desorbed than OP-mineral complexes (excluding IP that is occluded within the mineral matrix). Thereby, the dominant formation of the IP-mineral complexes with high mobility and solubility leads to the P availability in these soils (Study II).

In contrast, grassland soils exhibit significantly lower surface coverage by IP-mineral complexes in their fine fractions yet maintain similarly high available P (Study II). Considering the high coverage of OP-dominated compounds associated with SOM and the close correlation between TN and OP from Study I, the availability of P can be predominantly regulated by microbial mineralization/mobilization of N-rich OP compounds within MAOM, microbial biomass/necromass, and other OM constituents. Given the limited desorption rate of OP-mineral complexes, particularly those involving multiple phosphate groups through chelation with metal cations (Gerke, 2015) and multi-dentate ligand exchange reactions on mineral surfaces (Spohn, 2024; Strawn, 2021), microorganisms may preferentially target more accessible, C and N enriched OP compounds originating from microbial necromass and plant-derived by-products. This agrees with studies showing accelerated OP mineralization rates linked to microbial C demand in OC-rich grassland soils (Bünemann, 2015; Spohn and Kuzyakov, 2013). Thus, microbial processes facilitating the mineralization of these OP compounds significantly contribute to maintaining high P availability in grassland soils with high OC, TN and OP stocks (Fig. 4.1; Study I).

These two soils, under contrast land uses, exhibit distinct spatial distributions of IP and OP contents on microaggregate surfaces. The observation that OP dominated soils with high levels of OC and organic N achieve similar levels of P availability compared to IP-enriched soils underscores the potential of effectively utilizing the OP pool as a sustainable phosphorus management strategy, complementary to conventional IP fertilizer in temperate agricultural systems. In addition, the significantly higher OC and N stocks observed in grassland soils compared to cropland soils despite comparable P stocks and availability (Lei et al., 2025a) may highlight that efficient OP utilization depends on sufficient OC and N levels in the soil to sustain high microbial mineralization at comparable pH range, at which the P stabilization and organo-mineral stabilization mechanisms are similar. With IP dominated P pools in OM-poor cropland soils, the dominant formation of IP-mineral complexes is more prone to be loss via soil erosion due to less organo-mineral association (Quinton et al., 2010), increasing risks of particulate P loss and downslope eutrophication, which can be further exacerbated in IP dominates P pools. In contrast, OM-rich grassland soils demonstrate how mineral association with OM enhances aggregate formation, reducing erosion while stabilizing both OC and OP pools. The synergy between OM and phyllosilicates illustrated in this work offers two benefits for boosting P availability and mitigating P loss, which is particularly critical for sustainable P management on the hillslope facing a high risk of soil erosion. By enhancing OM retention at

proper pH ranges (slightly acidic to neutral pH ranges with proper microbial activity), temperate agroecosystems can simultaneously address P sustainability and soil conservation, aligning agricultural productivity with climate-smart purposes.

4.3 The role of phyllosilicates in maintaining carbon and phosphorus pools in temperate soils

The essential role of minerals in retaining OM, especially those clay-sized minerals, including phyllosilicates and oxides, has been widely recognized for carbon sequestration. They are the fundamental but most essential constituents of organo-mineral associations besides minor organo-organo associations that are resistant to biological decomposition (Kögel-Knabner et al., 2008; Possinger et al., 2020). The oxides have been regarded as highly correlated to carbon sequestration as well as P sink due to their higher specific surface areas, reactive sites and the ability to form stable inner-sphere complexes with OM and phosphate groups at proper pH ranges (Basinski et al., 2024; Gérard, 2016). However, on the other hand, the oxides only represent minor mineral composition in temperate soils (less than 10%) (Ito and Wagai, 2016), and can be even less (<5%) in those soils with limited weathering like Cambisols, Fluvisols, Leptosols, Histosols and Regosols (Ito and Wagai, 2016; Zech et al., 2022). Instead, the phyllosilicates, including 2:1 and 1:1 phyllosilicates, are the dominant clay minerals besides quartz in temperate soils (Ito and Wagai, 2016).

To better understand the role of phyllosilicates in retaining C and P in temperate zones, four representative soil types are chosen, including Cambisol, Luvisol, Fluvisol and Phaeozem (Study I, Study II). Cambisols and Luvisols dominate humid, mid-latitude zones and are intensively managed as cropland and grassland with generally sufficient phosphorus (Nortcliff, 2009; Zech et al., 2022). Phaeozems occur mainly in the ecotone between these humid regions and adjacent forest sites, while Fluvisols develop on periodically inundated flood plain landscapes throughout the temperate zone, where they accumulate large P reserves (Gocke et al., 2021; Zech et al., 2022).

To differentiate various forms of P on microaggregate surfaces and their association with distinct mineral types, this study introduces a novel method using NanoSIMS measurements based on two C-related channels and two P-related channels. Specifically, the $^{31}P^{16}O_2^-/(^{31}P^- + {}^{31}P^{16}O_2^-)$ ratio effectively distinguishes *myo*-inositol hexaphosphate from IP compounds, including Fe and Al phosphates. The $^{12}C^{14}N^-/(^{12}C^- + {}^{12}C^{14}N^-)$ ratio allows the differentiation of Gram-positive bacteria from IP compounds due to their distinct enrichment of N. This channel-ratio-based method thus enables precise differentiation of microregions dominated by different P compounds, facilitating better observation of organo-mineral associations on microaggregate surfaces.

The spatial distribution of C and different P compounds on microaggregate surfaces reveals that approximately 53% of P-associated regions are localized on OM-free phyllosilicate mineral surfaces, while phyllosilicates coated with OM account for an additional 34% of P associations (Fig. 4.5; Study II). Combined, these phyllosilicate-related regions represent over 85% of P retention on microaggregate surfaces. Although Al/Fe (hydr)oxides have traditionally been recognized as highly effective P-binding phases (Basinski et al., 2024; Gérard, 2016), their limited abundance (<2%) in these temperate soils, consistent with their globally reported low abundance in temperate topsoils (Ito and Wagai, 2016), suggests a limited role in P sorption in these soils. Consequently, the widespread occurrence and abundance of phyllosilicates compensate for their relatively lower intrinsic P-binding affinity, thus resulting in phyllosilicates as the primary P reservoirs in these temperate soils.

Importantly, the presence of OM associated with phyllosilicates may significantly enhance the P retention capacity. Although OM-associated regions covered only about 17% of the phyllosilicate surfaces, they contained approximately 34% of all P regions detected. (Fig. 4.5; Study II). Conversely, OM-free phyllosilicate surfaces, despite their dominance on microaggregate surfaces (~60%), account for only ~53% of the total P retention sites (Fig. 4.5; Study II). Thus, the unit P coverage on OM-associated phyllosilicates is approximately twice as high as that of OM-free phyllosilicates. This enhanced retention capacity is likely due to the higher specific surface areas and reactive sites per unit mass of OM compared to OM-free phyllosilicate surfaces (Strawn et al., 2019). These observations suggest that higher proportions of OM-associated phyllosilicates in soils, which are concentrated with OC, can significantly improve overall P retention potential, independent of high Al/Fe (hydr)oxide pools. Although previous studies have highlighted competitive sorption mechanisms between OM and P on mineral surfaces (Fink et al., 2016; Jindo et al., 2023), the NanoSIMS measurements reveal extensive co-occurrence rather than competitive exclusion of P and OM, suggesting a synergistic interaction widely existed.

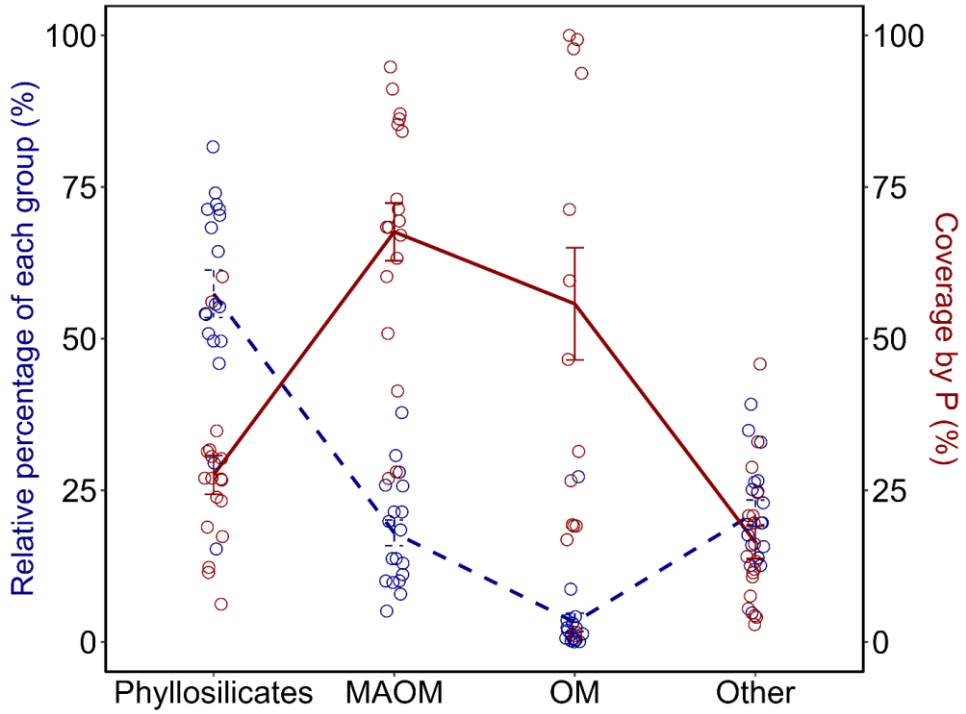

Fig. 4.5 The relative percentage of defined mineral groups and their respective coverage rate by P compounds. The red and blue lines and error bar show the relative abundance of each defined mineral group and their respective coverage by P compounds. Data are mean ± SE, n = 18. (Figure is taken and modified from Study II)

This study acknowledges specific methodological limitations of NanoSIMS, including its inability to fully resolve multilayer sorption and surface precipitation processes (Gérard, 2016) and challenges in quantifying absolute amounts at the pixel level, potentially leading to underestimates of mineral surface area complexities (Galili et al., 2023; Sayed and Polshettiwar, 2015). The absence of Al/Fe (hydr)oxides dominated regions on these soil microaggregates may be due to their limited abundance in these soils and the co-occurrence of Al/Fe (hydr)oxides with phyllosilicates in each pixel of NanoSIMS measurements. The smaller crystal size of Fe (hydr)oxides (15 ~ 40 nm for hematite and goethite by means) and their widely observed precipitation with Si-containing minerals in natural soil aggregates make them highly aggregated and hardly differentiated in temperate soils with a low amount of poorly crystallized Fe (hydr)oxides. Nonetheless, these findings suggest that the current perspective that emphasizes Al/Fe (hydr)oxides as the primary soil P retention phases in temperate soils (Amadou et al., 2022; Spohn, 2024; Strahm and Harrison, 2007) may be overemphasized in many soils, particularly in slightly acidic temperate soils. Instead, the direct observations on microaggregate surfaces indicate that phyllosilicates, especially when associated with OM, dominate soil P retention, which has been substantially underestimated. Given the low occurrence of Al/Fe (hydr)oxides documented in temperate soils (Ito and Wagai, 2016), their functional significance for P retention is limited. These insights emphasize the critical need to adjust soil P models by placing greater emphasis on phyllosilicate minerals in temperate soils

with the dominance of phyllosilicates within clay-sized minerals and underscores the critical role of OM in P retention benefit from phyllosilicate-OM associations, which can simultaneously enhance OC and P retention for climate-smart management options.

4.4 Silicate rock powder amendment as a strategy for long-term carbon sequestration for cropland soils

Silicate rock powder amendment is an emerging strategy for carbon dioxide removal (CDR) by storing atmospheric carbon dioxide (CO_2) as inorganic carbon (IC) in soil and aquatic systems (Seifritz, 1990). This enhanced rock weathering (ERW) strategy, first proposed by Seifritz (1990), has gained increasing attention in climate change mitigation discussions over recent decades (Beerling et al., 2025; Beerling et al., 2020; Bucka et al., 2024; Buckingham and Henderson, 2024; Buss et al., 2024a; Buss et al., 2024b; Clarkson et al., 2024; Hartmann et al., 2013; Hasemer et al., 2024; Kantola et al., 2017; Kelland et al., 2020; Köhler et al., 2010; Levy et al., 2024; Schuiling and Krijgsman, 2006; Sokol et al., 2024; Xu and Reinhard, 2025; Xu et al., 2024). Besides its potential for CDR, silicate rock powders enriched in macronutrients such as Ca, magnesium (Mg), sodium (Na), sulfur (S), P, and potassium (K) have also been used historically as soil amendments to enhance agricultural productivity and correct soil acidity (d'Hotman and Villiers, 1961; Gerth, 1939; Hilf, 1938; Leonardos, 1973; Leonardos et al., 1987; Swoboda et al., 2022). However, their efficiency as a CDR strategy and agricultural amendment depends significantly on soil types, plant species, rock types, particle sizes, and application rates (Swoboda et al., 2022). High application rates for CDR purposes may pose risks related to heavy metal contamination (Clarkson et al., 2024). Among various ERW materials, basalt is considered particularly cost-effective and abundant, with approximately 150 million tonnes (https://www.bgr.bund.de) in Germany, indicating its potential application across Germany.

The cropland soils investigated in Study I are slightly acidic and regularly amended with lime to increase soil alkalinity and maintain nutrient availability for agricultural productivity. To reverse the degraded OC stocks in these soils, ERW may be a strategy with multi-functions due to its theoretical function for soil acidity correction, enhanced carbon sequestration and nutrient supply. Therefore, to mechanistically understand the ERW effectiveness of these soils and predict their long-term carbon sequestration potential, two basalt materials (fresh and weathered basalt) are investigated.

Fresh basalt can similarly neutralize soil acidity through rapid neutralization of free protons (H^+) in the soil solution, as observed in Study III, reaching a pH level comparable to the level corrected by liming. Concurrently, the reaction of olivine with carbonic acid sequesters CO_2 within the soil solution as dissolved inorganic carbon (DIC), predominantly presented as

bicarbonate, within the typical pH range (Study I) of these soils. The buffering effect, generated by the release of dissolved Ca^{2+} and Mg^{2+} ions during olivine dissolution, promotes further accumulation of DIC following fresh basalt amendment (Study III). This accumulated DIC subsequently facilitates the formation of soil inorganic carbon (SIC) through precipitation with these dissolved cations derived from olivine dissolution.

However, significant reductions in soil organic carbon (SOC) content are concurrently observed in these slightly acidic topsoils amended with fresh basalt, mainly attributed to the elevated soil pH (Fig. 4.6, Study III), accompanied with the significant IC gain through the accumulation of DIC and SIC. Although pH-induced stimulation of OM decomposition is well-documented, such unintended OC losses pose critical questions for the large-scale deployment of ERW as a climate change mitigation strategy. The magnitude of SOC loss following fresh basalt amendment substantially exceeds the IC gained through olivine dissolution reactions, resulting in a net carbon loss from the soil after 6-months incubation (Study III).

In contrast, weathered basalt (referred to as ground weathered basalt in the following discussion, excluding 'weathered basalt' treatment mentioned in the Results section), characterized by olivine depletion, functions differently than fresh basalt. The absence of reactive olivine minerals reduced the rate of proton neutralization, thus causing minimal pH alteration and effectively preventing pH-driven SOC decomposition (Study III). Additionally, the increased specific surface area and abundance of exchangeable and dissolved Ca^{2+} associated with weathered basalt enhance the Ca-mediated OC stabilization. Reactions between carbonic acid and less reactive minerals, such as feldspar and pyroxene, lead to sustained SIC formation, as the DIC produced through dissolution of Ca-bearing minerals preferentially precipitated as Ca-carbonate within the soil (Study III). This directly results in no excess DIC leaching.

These contrasting carbon dynamics observed between fresh and weathered basalt highlight the complexities involved in assessing the long-term carbon sequestration potential associated with ERW. The theoretical oxide dissolution kinetics (Beerling et al., 2025; Beerling et al., 2020; Renforth, 2019) based estimation of ERW on carbon sequestration alone cannot well understand the interaction between SOC and IC, as the observation from Study III illustrate that initial OC losses resulting from pH elevation due to fresh basalt amendment can cause net C loss from the system.

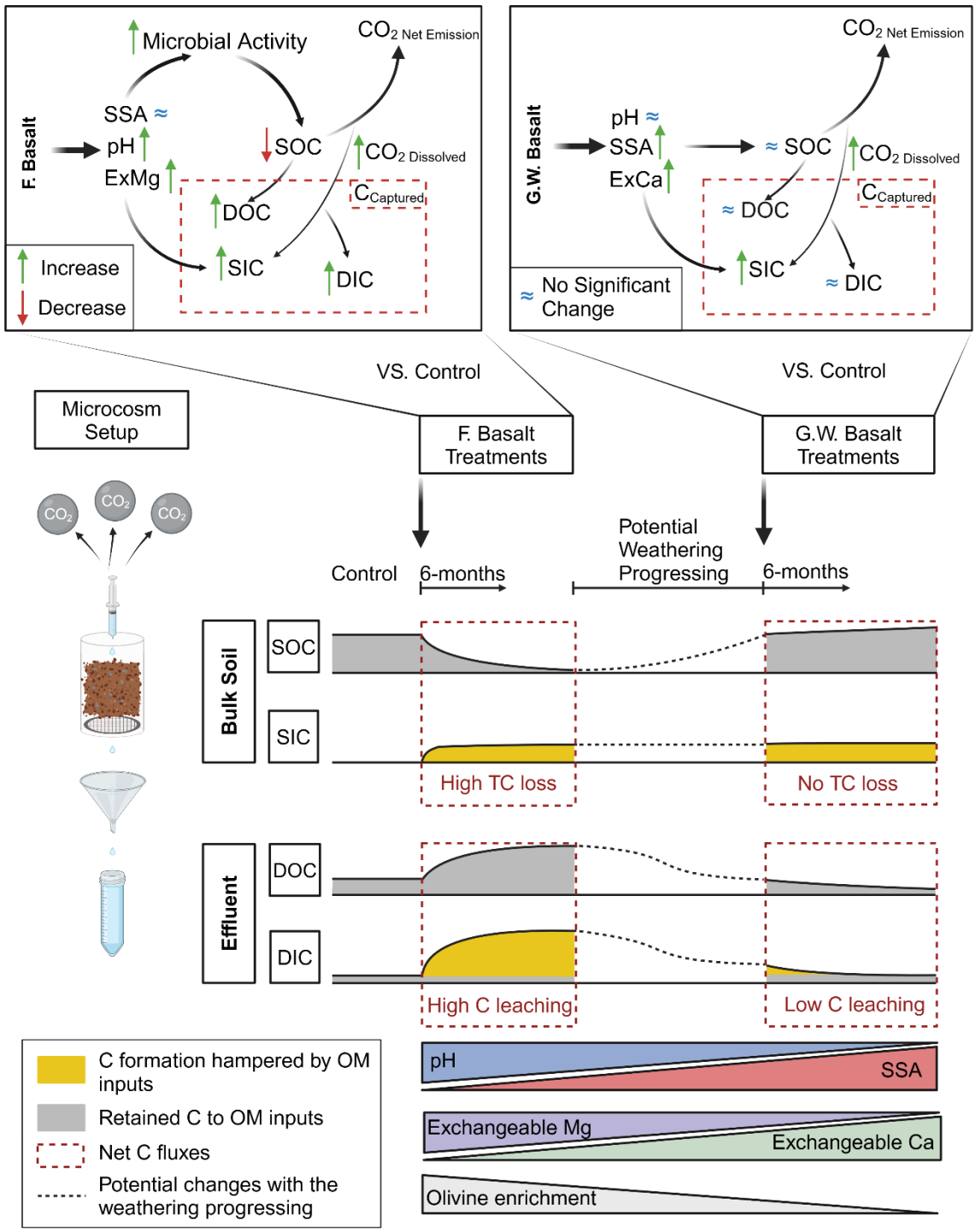

Fig. 4.6 Schematic graph of carbon fluxes within soil, atmosphere and effluent. Fresh basalt and ground weathered basalt treatments are compared to the control soils. The time-diagram shows changes in soil organic carbon (SOC), soil inorganic carbon (SIC), dissolved inorganic carbon (DIC) and dissolved organic carbon (DOC), as influenced by basalt weathering processes, relative to control soils. The 'ExCa', 'ExMg' and 'SSA' are referred to 'exchangeable Ca^{2+}', 'exchangeable Mg^{2+}' and 'specific surface area', respectively. (Figure is taken and modified from Study III)

With the weathering processing, due to the steady SIC formation at both olivine enriched (fresh basalt) and olivine depleted (weathered basalt) stages, the initial SOC loss may be offset over

extended periods. However, the prerequisite is the exclusion of additional new OM inputs from sources such as below- and above-ground biomass, anthropogenic organic fertilizers and organism residues. In practice, these cropland soils continuously receive new OM inputs. Decomposition of these new OM inputs generates additional acidity (free H^+ ions), competing with carbonic acid-driven dissolution of olivine and other Ca-rich minerals. Such competition can reduce the CDR effectiveness of basalt amendments (both fresh basalt and weathered basalt), as evidenced in Study III. During the 6-month incubation with only one-time new OM inputs, the diminishing DIC accumulation in the soil solution following fresh basalt amendment has been observed. At the same time, the depletion of SIC is observed with either fresh or weathered basalt treatments (Study III). In these slightly acidic cropland soils characterized by continuous new OM inputs, IC sequestration capacity is severely constrained, with less than 0.4% of the total carbon potentially sequestered as IC. Consequently, the primary benefit of silicate rock amendments under these conditions likely shifts toward enhancing SOC stabilization rather than significant IC gain.

In addition, with the aid of ^{13}C labelled straw, this study finds significant differences in new OM retention between fresh and weathered basalt amendments. Despite partial mitigation by soil acidification from decomposing OM, fresh basalt-induced pH elevation still significantly reduces its retention ability in soils. Conversely, weathered basalt, attributed to its marginal pH alteration, higher specific surface areas and higher exchangeable Ca, substantially improves the retention of new OC inputs (Study III). Furthermore, both fresh and weathered basalt consistently supply P to the soil, indicating their potential as a slow-released P fertilizer, as also reported by Bi et al. (2024).

In summary, this study estimates the potential carbon sequestration capacity associated with ERW to reverse the degraded C stocks in these cropland soils. Though significant amounts of C are stored as IC with the application of basalt materials, the effectiveness of carbon sequestration in these soils may not effectively function at the initial application phase, as observed SOC loss associated with fresh basalt amendments due to elevated soil pH via rapid H^+ neutralization. However, the long-term carbon sequestration promise in these soils is still convincing as the observed superior ability for both native and new OM retention in weathered basalt amendments besides its long-term IC accrual throughout weathering processes. Such mechanistic understanding thus suggests that silicate rock amendments might effectively replace lime in cropland soils where soil acidity mitigation is necessary due to the additional benefits of weathered basalt in SOC retention. This effectiveness of ERW is highly dependent on the balance between IC and OC pools and their interactions for climate change mitigation.

4.5 Implications for targeting climate-smart management options in temperate soils

Integrating the mechanistic studies discussed above with respect to the coupled OC, TN and P cycling in contrast land uses (Study I), divergent pathways for P retention and availability correlated with OC and N (Study II), as well as the carbon dynamics associated with emerging ERW strategy (Study III), several key mechanistic-based insights emerge for climate-smart management of temperate soils under cropland and grassland uses.

In extensively managed temperate grassland soils, regular organic fertilization and plant residues can sustain substantial stocks of OC, N, and P, particularly OP stocks. These soils function effectively as both C sinks and P reservoirs due to their well-preserved soil structure and continuous above- and belowground OM inputs (Study I). These maintained OM pools are especially crucial for hillslopes at risk of soil erosion and degradation as their association with mineral surfaces mitigates phosphorus losses through stable organo-mineral interactions. Meanwhile, high OM content ensures high availability of P via microbial immobilization processes driven by coupled OC and organic N cycling (Study II). Consequently, these soils support high productivity by sustaining adequate levels of available P with the least soil loss alongside their well-performed carbon sequestration capability.

Conversely, intensively managed temperate cropland soils receiving regular organic fertilization and lime amendments experience structural degradation and OM losses driven by continuous long-term ploughing and clear-harvest practices (Study I). The depletion of OM stocks results from less OM inputs, accelerated OM decomposition and soil erosion, leading to reduced soil fertility and a predominance of IP pools. Although high IP availability in these soils supports immediate agricultural productivity, they carry an elevated risk of phosphorus losses, contributing to the eutrophication of downstream aquatic systems (Study II). To reverse the degraded OM stocks, this work suggests that ERW strategy may be a promising climate-smart practice that serves not only as an alternative to lime for neutralizing soil acidity but also contributes to long-term CDR by forming IC pools. With weathering progress, the weathered ERW materials facilitate increased surface area and cation exchange capacity, fostering stable OC accumulation in MAOM fractions and enhancing carbon sequestration capacity (Study III).

Therefore, climate-smart management for temperate grassland soils under extensive use emphasizes minimal disturbance to preserve natural soil structure, maintaining optimal OC, N, and OP stoichiometry essential for sustained carbon sequestration and phosphorus availability. For temperate cropland soils subjected to intensive management, integrating organic amendments with ERW provides a mechanistically proven strategy that addresses critical agricultural needs such as soil acidity correction, nutrient replenishment, and enhanced carbon sequestration potential, thereby promoting soil productivity and ecological function.

5 Reference

Alt, F., Oelmann, Y., Herold, N., Schrumpf, M., Wilcke, W. (2011) Phosphorus partitioning in grassland and forest soils of Germany as related to land-use type, management intensity, and land use–related pH. Journal of Plant Nutrition and Soil Science 174, 195-209.

Amadou, I., Faucon, M.-P., Houben, D. (2022) New insights into sorption and desorption of organic phosphorus on goethite, gibbsite, kaolinite and montmorillonite. Applied Geochemistry 143, 105378.

Amann, T., Hartmann, J., Struyf, E., de Oliveira Garcia, W., Fischer, E.K., Janssens, I., Meire, P., Schoelynck, J. (2020) Enhanced Weathering and related element fluxes–a cropland mesocosm approach. Biogeosciences 17, 103-119.

Angst, G., Pokorný, J., Mueller, C.W., Prater, I., Preusser, S., Kandeler, E., Meador, T., Straková, P., Hájek, T., van Buiten, G. (2021) Soil texture affects the coupling of litter decomposition and soil organic matter formation. Soil Biology and Biochemistry 159, 108302.

Basinski, J.J., Bone, S.E., Klein, A.R., Thongsomboon, W., Mitchell, V., Shukle, J.T., Druschel, G.K., Thompson, A., Aristilde, L. (2024) Unraveling iron oxides as abiotic catalysts of organic phosphorus recycling in soil and sediment matrices. Nature Communications 15, 5930.

Beerling, D.J., Kantzas, E.P., Lomas, M.R., Taylor, L.L., Zhang, S., Kanzaki, Y., Eufrasio, R.M., Renforth, P., Mecure, J.-F., Pollitt, H. (2025) Transforming US agriculture for carbon removal with enhanced weathering. Nature, 1-10.

Beerling, D.J., Kantzas, E.P., Lomas, M.R., Wade, P., Eufrasio, R.M., Renforth, P., Sarkar, B., Andrews, M.G., James, R.H., Pearce, C.R. (2020) Potential for large-scale CO2 removal via enhanced rock weathering with croplands. Nature 583, 242-248.

Bi, B., Li, G., Goll, D.S., Lin, L., Chen, H., Xu, T., Chen, Q., Li, C., Wang, X., Hao, Z. (2024) Enhanced rock weathering increased soil phosphorus availability and altered root phosphorus-acquisition strategies. Global change biology 30, e17310.

Bollyn, J., Faes, J., Fritzsche, A., Smolders, E. (2017) Colloidal-bound polyphosphates and organic phosphates are bioavailable: a nutrient solution study. Journal of agricultural and food chemistry 65, 6762-6770.

Borrelli, P., Robinson, D.A., Fleischer, L.R., Lugato, E., Ballabio, C., Alewell, C., Meusburger, K., Modugno, S., Schütt, B., Ferro, V. (2017) An assessment of the global impact of 21st century land use change on soil erosion. Nature Communications 8, 2013.

Brady, N.C., Weil, R.R., Weil, R.R. (2008) The nature and properties of soils. Prentice Hall Upper Saddle River, NJ.

Brunauer, S., Emmett, P.H., Teller, E. (1938) Adsorption of gases in multimolecular layers. Journal of the American chemical society 60, 309-319.

Bucka, F.B., Guigue, J., Reifschneider, L., Pihlap, E., Garcia-Franco, N., Kühnel, A., Kögel-Knabner, I., Vidal, A. (2024) From waste to soil: Can we create functioning manufactured soils by recycling rock processing waste? Soil Use and Management 40, e13094.

Buckingham, F., Henderson, G. (2024) The enhanced weathering potential of a range of silicate and carbonate additions in a UK agricultural soil. Science of The Total Environment 907, 167701.

Bünemann, E.K. (2015) Assessment of gross and net mineralization rates of soil organic phosphorus–A review. Soil Biology and Biochemistry 89, 82-98.

Buss, W., Hasemer, H., Ferguson, S., Borevitz, J. (2024a) Stabilisation of soil organic matter with rock dust partially counteracted by plants. Global change biology 30, e17052.

Buss, W., Hasemer, H., Sokol, N.W., Rohling, E.J., Borevitz, J. (2024b) Applying minerals to soil to draw down atmospheric carbon dioxide through synergistic organic and inorganic pathways. Communications Earth & Environment 5, 602.

Cade-Menun, B.J. (2017) Characterizing phosphorus forms in cropland soils with solution 31 P-NMR: past studies and future research needs. Chemical and Biological Technologies in Agriculture 4, 1-12.

Celi, L., De Luca, G., Barberis, E. (2003) Effects of interaction of organic and inorganic P with ferrihydrite and kaolinite-iron oxide systems on iron release. Soil science 168, 479-488.

Chaopricha, N.T., Marín-Spiotta, E. (2014) Soil burial contributes to deep soil organic carbon storage. Soil Biology and Biochemistry 69, 251-264.

Chaplot, V., Poesen, J. (2012) Sediment, soil organic carbon and runoff delivery at various spatial scales. Catena 88, 46-56.

Chenu, C., Plante, A. (2006) Clay-sized organo-mineral complexes in a cultivation chronosequence: revisiting the concept of the 'primary organo-mineral complex'. European journal of soil science 57, 596-607.

Christensen, B.T., (1996) Matching measurable soil organic matter fractions with conceptual pools in simulation models of carbon turnover: revision of model structure, Evaluation of soil organic matter models: using existing long-term datasets. Springer, pp. 143-159.

Christensen, H., Griffiths, B., Christensen, S. (1992) Bacterial incorporation of tritiated thymidine and populations of bacteriophagous fauna in the rhizosphere of wheat. Soil Biology and Biochemistry 24, 703-709.

Clarkson, M.O., Larkin, C.S., Swoboda, P., Reershemius, T., Suhrhoff, T.J., Maesano, C.N., Campbell, J.S. (2024) A review of measurement for quantification of carbon dioxide removal by enhanced weathering in soil. Frontiers in Climate 6, 1345224.

Cleveland, C.C., Liptzin, D. (2007) C: N: P stoichiometry in soil: is there a "Redfield ratio" for the microbial biomass? Biogeochemistry 85, 235-252.

Condron, L.M., Turner, B.L., Cade-Menun, B.J. (2005) Chemistry and dynamics of soil organic phosphorus. Phosphorus: agriculture and the environment 46, 87-121.

Cordell, D., White, S. (2011) Peak phosphorus: clarifying the key issues of a vigorous debate about long-term phosphorus security. Sustainability 3, 2027-2049.

Cotrufo, M.F., Ranalli, M.G., Haddix, M.L., Six, J., Lugato, E. (2019) Soil carbon storage informed by particulate and mineral-associated organic matter. Nature Geoscience 12, 989-994.

D'Elia, A.H., Liles, G.C., Viers, J.H., Smart, D.R. (2017) Deep carbon storage potential of buried floodplain soils. Scientific reports 7, 8181.

d'Hotman, D., Villiers, O. (1961) Soil rejuvenation with crushed basalt in Mauritius. Int. Sugar J 63, 363-364.

Darch, T., Blackwell, M., Hawkins, J., Haygarth, P., Chadwick, D. (2014) A meta-analysis of organic and inorganic phosphorus in organic fertilizers, soils, and water: implications for water quality. Critical Reviews in Environmental Science and Technology 44, 2172-2202.

Dietzen, C., Harrison, R., Michelsen-Correa, S. (2018) Effectiveness of enhanced mineral weathering as a carbon sequestration tool and alternative to agricultural lime: an incubation experiment. International Journal of Greenhouse Gas Control 74, 251-258.

Doetterl, S., Berhe, A.A., Heckman, K., Lawrence, C., Schnecker, J., Vargas, R., Vogel, C., Wagai, R. (2025) A landscape-scale view of soil organic matter dynamics. Nature Reviews Earth & Environment, 1-15.

Drever, J., Stillings, L. (1997) The role of organic acids in mineral weathering. Colloids and Surfaces A: physicochemical and engineering aspects 120, 167-181.

Eusterhues, K., Thieme, J., Narvekar, S., Araki, T., Kazemian, M., Kaulich, B., Regier, T., Wang, J., Lugmeier, J., Höschen, C. (2023) Importance of inner-sphere PO-Fe bonds in natural and synthetic mineral-organic associations. Science of The Total Environment 905, 167232.

Fang, H., Cui, Z., He, G., Huang, L., Chen, M. (2017) Phosphorus adsorption onto clay minerals and iron oxide with consideration of heterogeneous particle morphology. Science of The Total Environment 605, 357-367.

Fanin, N., Hättenschwiler, S., Schimann, H., Fromin, N. (2015) Interactive effects of C, N and P fertilization on soil microbial community structure and function in an A mazonian rain forest. Functional Ecology 29, 140-150.

Fink, J.R., Inda, A.V., Tiecher, T., Barrón, V. (2016) Iron oxides and organic matter on soil phosphorus availability. Ciencia e agrotecnologia 40, 369-379.

Fu, X., Shao, M., Wei, X., Horton, R. (2010) Soil organic carbon and total nitrogen as affected by vegetation types in Northern Loess Plateau of China. Geoderma 155, 31-35.

Galili, N., Kaplan-Ashiri, I., Halevy, I. (2023) Cathodoluminescence of iron oxides and oxyhydroxides. American Mineralogist 108, 1436-1448.

George, T.S., Giles, C.D., Menezes-Blackburn, D., Condron, L.M., Gama-Rodrigues, A.C., Jaisi, D., Lang, F., Neal, A.L., Stutter, M.I., Almeida, D.S. (2018) Organic phosphorus in the terrestrial environment: a perspective on the state of the art and future priorities. Plant and Soil 427, 191-208.

Gérard, F. (2016) Clay minerals, iron/aluminum oxides, and their contribution to phosphate sorption in soils—A myth revisited. Geoderma 262, 213-226.

Gerke, J. (2015) Phytate (inositol hexakisphosphate) in soil and phosphate acquisition from inositol phosphates by higher plants. A review. Plants 4, 253-266.

Gerth, G. (1939) The possibilities of rock meal as a soil improver, and their significance for the rock-quarrying industries.

Gocke, M.I., Don, A., Heidkamp, A., Schneider, F., Amelung, W. (2021) The phosphorus status of German cropland—An inventory of top-and subsoils. Journal of Plant Nutrition and Soil Science 184, 51-64.

Goss, M.J., Oliver, M.A. (2023) Encyclopedia of Soils in the Environment. Elsevier.

Griffiths, B.S., Spilles, A., Bonkowski, M. (2012) C: N: P stoichiometry and nutrient limitation of the soil microbial biomass in a grazed grassland site under experimental P limitation or excess. Ecological Processes 1, 1-11.

Guo, L.B., Gifford, R.M. (2002) Soil carbon stocks and land use change: a meta analysis. Global change biology 8, 345-360.

Hamza, M., Anderson, W.K. (2005) Soil compaction in cropping systems: A review of the nature, causes and possible solutions. Soil and Tillage Research 82, 121-145.

Haque, F., Khalidy, R., Chiang, Y.W., Santos, R.M. (2023) Constraining the capacity of global croplands to CO2 drawdown via mineral weathering. ACS Earth and Space Chemistry 7, 1294-1305.

Haque, F., Santos, R.M., Chiang, Y.W. (2020) CO2 sequestration by wollastonite-amended agricultural soils–An Ontario field study. International Journal of Greenhouse Gas Control 97, 103017.

Haque, F., Santos, R.M., Dutta, A., Thimmanagari, M., Chiang, Y.W. (2019) Co-benefits of wollastonite weathering in agriculture: CO2 sequestration and promoted plant growth. ACS omega 4, 1425-1433.

Hartmann, J., West, A.J., Renforth, P., Köhler, P., De La Rocha, C.L., Wolf-Gladrow, D.A., Dürr, H.H., Scheffran, J. (2013) Enhanced chemical weathering as a geoengineering strategy to reduce atmospheric carbon dioxide, supply nutrients, and mitigate ocean acidification. Reviews of Geophysics 51, 113-149.

Hasemer, H., Borevitz, J., Buss, W. (2024) Measuring enhanced weathering: inorganic carbon-based approaches may be required to complement cation-based approaches. Frontiers in Climate 6, 1352825.

Hedley, M.J., Stewart, J., Chauhan, B.S. (1982) Changes in inorganic and organic soil phosphorus fractions induced by cultivation practices and by laboratory incubations. Soil Science Society of America Journal 46, 970-976.

Heuck, C., Weig, A., Spohn, M. (2015) Soil microbial biomass C: N: P stoichiometry and microbial use of organic phosphorus. Soil Biology and Biochemistry 85, 119-129.

Hilf, H. (1938) The manuring of poor sands with basalt grit.

Hoffmann, T., Schlummer, M., Notebaert, B., Verstraeten, G., Korup, O. (2013) Carbon burial in soil sediments from Holocene agricultural erosion, Central Europe. Global Biogeochemical Cycles 27, 828-835.

Ito, A., Wagai, R. (2016) Global map of clay minerals in terrestrial soils. PANGAEA.

Jindo, K., Audette, Y., Olivares, F.L., Canellas, L.P., Smith, D.S., Paul Voroney, R. (2023) Biotic and abiotic effects of soil organic matter on the phytoavailable phosphorus in soils: A review. Chemical and Biological Technologies in Agriculture 10, 29.

Just, C., Poeplau, C., Don, A., van Wesemael, B., Kögel-Knabner, I., Wiesmeier, M. (2021) A simple approach to isolate slow and fast cycling organic carbon fractions in central European soils—Importance of dispersion method. Frontiers in Soil Science 1, 692583.

Kantola, I.B., Masters, M.D., Beerling, D.J., Long, S.P., DeLucia, E.H. (2017) Potential of global croplands and bioenergy crops for climate change mitigation through deployment for enhanced weathering. Biology letters 13, 20160714.

Kautz, T., Amelung, W., Ewert, F., Gaiser, T., Horn, R., Jahn, R., Javaux, M., Kemna, A., Kuzyakov, Y., Munch, J.-C. (2013) Nutrient acquisition from arable subsoils in temperate climates: a review. Soil Biology and Biochemistry 57, 1003-1022.

Kelland, M.E., Wade, P.W., Lewis, A.L., Taylor, L.L., Sarkar, B., Andrews, M.G., Lomas, M.R., Cotton, T.A., Kemp, S.J., James, R.H. (2020) Increased yield and CO2 sequestration potential with the C4 cereal Sorghum bicolor cultivated in basaltic rock dust-amended agricultural soil. Global change biology 26, 3658-3676.

Khan, A.A., Jilani, G., Akhtar, M.S., Naqvi, S.M.S., Rasheed, M. (2009) Phosphorus solubilizing bacteria: occurrence, mechanisms and their role in crop production. J. agric. biol. sci 1, 48-58.

Khan, K.S., Joergensen, R.G. (2019) Stoichiometry of the soil microbial biomass in response to amendments with varying C/N/P/S ratios. Biology and fertility of Soils 55, 265-274.

Kirkby, C., Kirkegaard, J., Richardson, A., Wade, L., Blanchard, C., Batten, G. (2011) Stable soil organic matter: a comparison of C: N: P: S ratios in Australian and other world soils. Geoderma 163, 197-208.

Klemme, A., Rixen, T., Müller, M., Notholt, J., Warneke, T. (2022) Destabilization of carbon in tropical peatlands by enhanced weathering. Communications Earth & Environment 3, 212.

Kögel-Knabner, I. (2002) The macromolecular organic composition of plant and microbial residues as inputs to soil organic matter. Soil Biology and Biochemistry 34, 139-162.

Kögel-Knabner, I., Amelung, W. (2021) Soil organic matter in major pedogenic soil groups. Geoderma 384, 114785.

Kögel-Knabner, I., Guggenberger, G., Kleber, M., Kandeler, E., Kalbitz, K., Scheu, S., Eusterhues, K., Leinweber, P. (2008) Organo-mineral associations in temperate soils: Integrating biology, mineralogy, and organic matter chemistry. Journal of Plant Nutrition and Soil Science 171, 61-82.

Köhler, P., Hartmann, J., Wolf-Gladrow, D.A. (2010) Geoengineering potential of artificially enhanced silicate weathering of olivine. Proceedings of the National Academy of Sciences 107, 20228-20233.

Kölbl, A., Leifeld, J., Kögel-Knabner, I. (2005) A comparison of two methods for the isolation of free and occluded particulate organic matter. Journal of Plant Nutrition and Soil Science 168, 660-667.

Kopittke, P.M., Dalal, R.C., Finn, D., Menzies, N.W. (2017) Global changes in soil stocks of carbon, nitrogen, phosphorus, and sulphur as influenced by long-term agricultural production. Global change biology 23, 2509-2519.

Kruse, J., Abraham, M., Amelung, W., Baum, C., Bol, R., Kühn, O., Lewandowski, H., Niederberger, J., Oelmann, Y., Rüger, C. (2015) Innovative methods in soil phosphorus research: A review. Journal of Plant Nutrition and Soil Science 178, 43-88.

Larson, R., Albert, A., Walker, J. (1938) Soil reaction in relation to Potato scab.

Lavallee, J.M., Soong, J.L., Cotrufo, M.F. (2020) Conceptualizing soil organic matter into particulate and mineral-associated forms to address global change in the 21st century. Global change biology 26, 261-273.

Lefebvre, D., Goglio, P., Williams, A., Manning, D.A., De Azevedo, A.C., Bergmann, M., Meersmans, J., Smith, P. (2019) Assessing the potential of soil carbonation and enhanced weathering through Life Cycle Assessment: A case study for Sao Paulo State, Brazil. Journal of Cleaner Production 233, 468-481.

Lei, K., Bucka, F.B., Just, C., van Grinsven, S., Floßmann, S., Dannenmann, M., Völkel, J., Kögel-Knabner, I. (2025a) Distinct impact of land use and soil development processes on coupled biogeochemical cycling of C, N and P in a temperate hillslope-flood plain system. Biogeochemistry 168, 21.

Lei, K., Bucka, F.B., Teixeira, P.P., Buegger, F., Just, C., Kögel-Knabner, I. (2025b) Balancing Organic and Inorganic Carbon Dynamics in Enhanced Rock Weathering: Implications for Carbon Sequestration. Global change biology 31, e70186.

Leonardos, O.H. (1973) The Origin and Alteration of Granitic Rocks in Brazil: A Study of Metamorphism, Anatexis, Weathering and Soil Fertility Within Granitic Terrain in Eastern Brazil. The University of Manchester (United Kingdom).

Leonardos, O.H., Fyfe, W., Kronberg, B. (1987) The use of ground rocks in laterite systems: an improvement to the use of conventional soluble fertilizers? Chemical Geology 60, 361-370.

Levy, C.R., Almaraz, M., Beerling, D.J., Raymond, P., Reinhard, C.T., Suhrhoff, T.J., Taylor, L. (2024) Enhanced rock weathering for carbon removal–monitoring and mitigating potential environmental impacts on agricultural land. Environmental Science & Technology 58, 17215-17226.

Li, C., Chen, X., Jia, Z., Zhai, L., Zhang, B., Grüters, U., Ma, S., Qian, J., Liu, X., Zhang, J. (2024) Meta-analysis reveals the effects of microbial inoculants on the biomass and diversity of soil microbial communities. Nature Ecology & Evolution 8, 1270-1284.

Li, K., Sinha, B., Hoppe, P. (2016) Speciation of nitrogen-bearing species using negative and positive secondary ion spectra with nano secondary ion mass spectrometry. Analytical chemistry 88, 3281-3288.

Li, Q., Chang, J., Li, L., Lin, X., Li, Y. (2023) Research progress of nano-scale secondary ion mass spectrometry (NanoSIMS) in soil science: evolution, applications, and challenges. Science of The Total Environment 905, 167257.

Malherbe, J., Penen, F., Isaure, M.-P., Frank, J., Hause, G., Dobritzsch, D., Gontier, E., Horréard, F.o., Hillion, F.o., Schaumlöffel, D. (2016) A new radio frequency plasma oxygen primary ion source on nano secondary ion mass spectrometry for improved lateral resolution and detection of electropositive elements at single cell level. Analytical chemistry 88, 7130-7136.

Martin, M., Celi, L., Barberis, E. (2004) Desorption and plant availability of myo-inositol hexaphosphate adsorbed on goethite. Soil science 169, 115-124.

Martínez-Cuesta, R., Holmer, A., Buegger, F., Dannenmann, M., Schloter, M., Schulz, S. (2025) Land use drives prokaryotic community composition of directly adjacent grasslands. Biology and Fertility of Soils 61, 71-84.

Martínez-Mena, M., Almagro, M., García-Franco, N., de Vente, J., García, E., Boix-Fayos, C. (2019) Fluvial sedimentary deposits as carbon sinks: organic carbon pools and stabilization mechanisms across a Mediterranean catchment. Biogeosciences 16, 1035-1051.

Mayer, S., Kühnel, A., Burmeister, J., Kögel-Knabner, I., Wiesmeier, M. (2019) Controlling factors of organic carbon stocks in agricultural topsoils and subsoils of Bavaria. Soil and Tillage Research 192, 22-32.

Mayer, S., Schwindt, D., Steffens, M., Völkel, J., Kögel-Knabner, I. (2018) Drivers of organic carbon allocation in a temperate slope-floodplain catena under agricultural use. Geoderma 327, 63-72.

Mew, M., Steiner, G., Haneklaus, N., Geissler, B. (2023) Phosphate price peaks and negotiations–Part 2: The 2008 peak and implications for the future. Resources Policy 83, 103588.

Midwood, A., Boutton, T. (1998) Soil carbonate decomposition by acid has little effect on δ13C of organic matter. Soil Biology and Biochemistry 30, 1301-1307.

Müller, T.S., Dechow, R., Flessa, H. (2022) Inventory and assessment of pH in cropland and grassland soils in Germany#. Journal of Plant Nutrition and Soil Science 185, 145-158.

Nel, T., Bruneel, Y., Smolders, E. (2023) Comparison of five methods to determine the cation exchange capacity of soil. Journal of Plant Nutrition and Soil Science 186, 311-320.

Nortcliff, S. (2009) The soil: nature, sustainable use, management, and protection–an overview. Gaia-Ecological Perspectives for Science and Society 18, 58-68.

Oelkers, E.H., Declercq, J., Saldi, G.D., Gislason, S.R., Schott, J. (2018) Olivine dissolution rates: A critical review. Chemical Geology 500, 1-19.

Olsen, S.R. (1954) Estimation of available phosphorus in soils by extraction with sodium bicarbonate. US Department of Agriculture.

Omoike, A., Chorover, J. (2006) Adsorption to goethite of extracellular polymeric substances from Bacillus subtilis. Geochimica et Cosmochimica Acta 70, 827-838.

Page, A.L. (1982) Methods of soil analysis. Part 2. Chemical and microbiological properties.

Poeplau, C., Don, A., Vesterdal, L., Leifeld, J., Van Wesemael, B., Schumacher, J., Gensior, A. (2011) Temporal dynamics of soil organic carbon after land-use change in the temperate zone–carbon response functions as a model approach. Global change biology 17, 2415-2427.

Possinger, A.R., Zachman, M.J., Enders, A., Levin, B.D., Muller, D.A., Kourkoutis, L.F., Lehmann, J. (2020) Organo–organic and organo–mineral interfaces in soil at the nanometer scale. Nature Communications 11, 6103.

Power, I.M., Dipple, G.M., Bradshaw, P.M., Harrison, A.L. (2020) Prospects for CO2 mineralization and enhanced weathering of ultramafic mine tailings from the Baptiste nickel deposit in British Columbia, Canada. International Journal of Greenhouse Gas Control 94, 102895.

Power, I.M., Paulo, C., Rausis, K. (2023) The mining industry's role in enhanced weathering and mineralization for CO2 removal. Environmental Science & Technology 58, 43-53.

Prout, J.M., Shepherd, K.D., McGrath, S.P., Kirk, G.J., Haefele, S.M. (2021) What is a good level of soil organic matter? An index based on organic carbon to clay ratio. European journal of soil science 72, 2493-2503.

Quinton, J.N., Govers, G., Van Oost, K., Bardgett, R.D. (2010) The impact of agricultural soil erosion on biogeochemical cycling. Nature Geoscience 3, 311-314.

Renforth, P. (2019) The negative emission potential of alkaline materials. Nature Communications 10, 1401.

Ritschel, T., Aehnelt, M., Totsche, K.U. (2023) Organic matter governs weathering rates and microstructure evolution during early pedogenesis. Geoderma 429, 116269.

Rumpel, C., Kögel-Knabner, I. (2011) Deep soil organic matter—a key but poorly understood component of terrestrial C cycle. Plant and Soil 338, 143-158.

Sayed, F.N., Polshettiwar, V. (2015) Facile and sustainable synthesis of shaped iron oxide nanoparticles: effect of iron precursor salts on the shapes of iron oxides. Scientific reports 5, 9733.

Schad, P., Dondeyne, S. (2016) World reference base for soil resources.

Schiedung, M., Barré, P., Peoplau, C. (2025) Separating fast from slow cycling soil organic carbon–A multi-method comparison on land use change sites. Geoderma 453, 117154.

Schleuss, P.-M., Widdig, M., Biederman, L.A., Borer, E.T., Crawley, M.J., Kirkman, K.P., Seabloom, E.W., Wragg, P.D., Spohn, M. (2021) Microbial substrate stoichiometry governs nutrient effects on nitrogen cycling in grassland soils. Soil Biology and Biochemistry 155, 108168.

Schmidt, M.W., Torn, M.S., Abiven, S., Dittmar, T., Guggenberger, G., Janssens, I.A., Kleber, M., Kögel-Knabner, I., Lehmann, J., Manning, D.A. (2011) Persistence of soil organic matter as an ecosystem property. Nature 478, 49-56.

Scholz, R.W., Wellmer, F.-W., Mew, M., Steiner, G. (2025) The dynamics of increasing mineral resources and improving resource efficiency: Prospects for mid-and long-term security of phosphorus supply. Resources, Conservation and Recycling 213, 107993.

Schuiling, R., Krijgsman, P. (2006) Enhanced weathering: an effective and cheap tool to sequester CO2. Climatic Change 74, 349-354.

Seifritz, W. (1990) CO2 disposal by means of silicates. Nature 345, 486-486.

Sigua, G.C., Coleman, S.W. (2010) Spatial distribution of soil carbon in pastures with cow-calf operation: effects of slope aspect and slope position. Journal of Soils and Sediments 10, 240-247.

Six, J., Elliott, E., Paustian, K., Doran, J. (1998) Aggregation and soil organic matter accumulation in cultivated and native grassland soils. Soil Science Society of America Journal 62, 1367-1377.

Sokol, N.W., Sohng, J., Moreland, K., Slessarev, E., Goertzen, H., Schmidt, R., Samaddar, S., Holzer, I., Almaraz, M., Geoghegan, E. (2024) Reduced accrual of mineral-associated organic matter after two years of enhanced rock weathering in cropland soils, though no net losses of soil organic carbon. Biogeochemistry 167, 989-1005.

Spohn, M. (2020a) Increasing the organic carbon stocks in mineral soils sequesters large amounts of phosphorus. Global change biology 26, 4169-4177.

Spohn, M. (2020b) Phosphorus and carbon in soil particle size fractions: A synthesis. Biogeochemistry 147, 225-242.

Spohn, M. (2024) Preferential adsorption of nitrogen-and phosphorus-containing organic compounds to minerals in soils: A review. Soil Biology and Biochemistry, 109428.

Spohn, M., Giani, L. (2011) Impacts of land use change on soil aggregation and aggregate stabilizing compounds as dependent on time. Soil Biology and Biochemistry 43, 1081-1088.

Spohn, M., Kuzyakov, Y. (2013) Distribution of microbial-and root-derived phosphatase activities in the rhizosphere depending on P availability and C allocation–Coupling soil zymography with 14C imaging. Soil Biology and Biochemistry 67, 106-113.

Stewart, J., Tiessen, H. (1987) Dynamics of soil organic phosphorus. Biogeochemistry 4, 41-60.

Strahm, B.D., Harrison, R.B. (2007) Mineral and organic matter controls on the sorption of macronutrient anions in variable-charge soils. Soil Science Society of America Journal 71, 1926-1933.

Strawn, D.G. (2021) Sorption mechanisms of chemicals in soils. Soil Systems 5, 13.

Strawn, D.G., Bohn, H.L., O'Connor, G.A. (2019) Soil chemistry. John Wiley & Sons.

Stutter, M.I., Shand, C.A., George, T.S., Blackwell, M.S., Dixon, L., Bol, R., MacKay, R.L., Richardson, A.E., Condron, L.M., Haygarth, P.M. (2015) Land use and soil factors affecting accumulation of phosphorus species in temperate soils. Geoderma 257, 29-39.

Sulieman, S., Mühling, K.H. (2021) Utilization of soil organic phosphorus as a strategic approach for sustainable agriculture. Journal of Plant Nutrition and Soil Science 184, 311-319.

Sun, Y., Wang, C., Chen, X., Liu, S., Lu, X., Chen, H.Y., Ruan, H. (2022) Phosphorus additions imbalance terrestrial ecosystem C: N: P stoichiometry. Global change biology 28, 7353-7365.

Sutfin, N.A., Wohl, E.E., Dwire, K.A. (2016) Banking carbon: a review of organic carbon storage and physical factors influencing retention in floodplains and riparian ecosystems. Earth Surface Processes and Landforms 41, 38-60.

Swoboda, P., Döring, T.F., Hamer, M. (2022) Remineralizing soils? The agricultural usage of silicate rock powders: A review. Science of The Total Environment 807, 150976.

te Pas, E.E., Hagens, M., Comans, R.N. (2023) Assessment of the enhanced weathering potential of different silicate minerals to improve soil quality and sequester CO2. Frontiers in Climate 4, 954064.

Tipping, E., Somerville, C.J., Luster, J. (2016) The C: N: P: S stoichiometry of soil organic matter. Biogeochemistry 130, 117-131.

Totsche, K.U., Amelung, W., Gerzabek, M.H., Guggenberger, G., Klumpp, E., Knief, C., Lehndorff, E., Mikutta, R., Peth, S., Prechtel, A. (2018) Microaggregates in soils. Journal of Plant Nutrition and Soil Science 181, 104-136.

Turner, B.L., Lambers, H., Condron, L.M., Cramer, M.D., Leake, J.R., Richardson, A.E., Smith, S.E. (2013) Soil microbial biomass and the fate of phosphorus during long-term ecosystem development. Plant and Soil 367, 225-234.

Tyner, E.H. (1940) The use of sodium metaphosphate for dispersion of soils for mechanical analysis.

Umwelt, B.L.f. (2024) Digitale Geologische Karte 1: 25.000 (dGK25). Umwelt Atlas. www. umweltatlas. bayern. de.

Van Oost, K., Quine, T., Govers, G., De Gryze, S., Six, J., Harden, J., Ritchie, J., McCarty, G., Heckrath, G., Kosmas, C. (2007) The impact of agricultural soil erosion on the global carbon cycle. Science 318, 626-629.

Van Straaten, P. (2007) Agrogeology: the use of rocks for crops.

Vicca, S., Goll, D.S., Hagens, M., Hartmann, J., Janssens, I.A., Neubeck, A., Peñuelas, J., Poblador, S., Rijnders, J., Sardans, J. (2022) Is the climate change mitigation effect of enhanced silicate weathering governed by biological processes? Global change biology 28, 711-726.

Vidal, A., Klöffel, T., Guigue, J., Angst, G., Steffens, M., Hoeschen, C., Mueller, C.W. (2021) Visualizing the transfer of organic matter from decaying plant residues to soil mineral surfaces controlled by microorganisms. Soil Biology and Biochemistry 160, 108347.

Völkel, J. (1995) Periglaziale Deckschichten und Böden im Bayerischen Wald und seinen Randgebieten als geogene Grundlagen landschaftsökologischer Forschung im Bereich naturnaher Waldstandorte.

von Lützow, M., Kögel-Knabner, I., Ludwig, B., Matzner, E., Flessa, H., Ekschmitt, K., Guggenberger, G., Marschner, B., Kalbitz, K. (2008) Stabilization mechanisms of organic matter in four temperate soils: Development and application of a conceptual model. Journal of Plant Nutrition and Soil Science 171, 111-124.

Von Sperber, C., Stallforth, R., Du Preez, C., Amelung, W. (2017) Changes in soil phosphorus pools during prolonged arable cropping in semiarid grasslands. European journal of soil science 68, 462-471.

Walker, T., Adams, A. (1958) Studies on soil organic matter: I. Influence of phosphorus content of parent materials on accumulations of carbon, nitrogen, sulfur, and organic phosphorus in grassland soils. Soil science 85, 307-318.

Wang, C., Kuzyakov, Y. (2024) Soil organic matter priming: The pH effects. Global change biology 30, e17349.

Wang, J.L., Liu, K.L., Zhao, X.Q., Zhang, H.Q., Li, D., Li, J.J., Shen, R.F. (2021) Balanced fertilization over four decades has sustained soil microbial communities and improved soil fertility and rice productivity in red paddy soil. Science of The Total Environment 793, 148664.

Weihrauch, C., Weber, C.J. (2021) Comparative risk assessment of phosphorus loss from “deep phosphorus stocks” in floodplain subsoils to surface waters. Science of The Total Environment 796, 149037.

Wiesmeier, M., Barthold, F., Spörlein, P., Geuß, U., Hangen, E., Reischl, A., Schilling, B., Angst, G., von Lützow, M., Kögel-Knabner, I. (2014) Estimation of total organic carbon storage and its driving factors in soils of Bavaria (southeast Germany). Geoderma Regional 1, 67-78.

Wiesmeier, M., Mayer, S., Burmeister, J., Hübner, R., Kögel-Knabner, I. (2020) Feasibility of the 4 per 1000 initiative in Bavaria: A reality check of agricultural soil management and carbon sequestration scenarios. Geoderma 369, 114333.

Wiesmeier, M., Spörlein, P., Geuß, U., Hangen, E., Haug, S., Reischl, A., Schilling, B., von Lützow, M., Kögel-Knabner, I. (2012) Soil organic carbon stocks in southeast Germany (Bavaria) as affected by land use, soil type and sampling depth. Global change biology 18, 2233-2245.

Wiesmeier, M., von Lützow, M., Spörlein, P., Geuß, U., Hangen, E., Reischl, A., Schilling, B., Kögel-Knabner, I. (2015) Land use effects on organic carbon storage in soils of Bavaria: the importance of soil types. Soil and Tillage Research 146, 296-302.

Williams, C., Steinbergs, A. (1959) Soil sulphur fractions as chemical indices of available sulphur in some Australian soils. Australian Journal of Agricultural Research 10, 340-352.

Wu, R., Tiessen, H. (2002) Effect of land use on soil degradation in alpine grassland soil, China. Soil Science Society of America Journal 66, 1648-1655.

Xu, P., Reinhard, C.T. (2025) Evaluating the carbon capture potential of industrial waste as a feedstock for enhanced weathering. Environmental Research Letters 20, 044013.

Xu, T., Yuan, Z., Vicca, S., Goll, D.S., Li, G., Lin, L., Chen, H., Bi, B., Chen, Q., Li, C. (2024) Enhanced silicate weathering accelerates forest carbon sequestration by stimulating the soil mineral carbon pump. Global change biology 30, e17464.

Xu, X., Thornton, P.E., Post, W.M. (2013) A global analysis of soil microbial biomass carbon, nitrogen and phosphorus in terrestrial ecosystems. Global Ecology and Biogeography 22, 737-749.

Zech, W., Schad, P., Hintermaier-Erhard, G. (2022) Soils of the World. Springer-Verlag.

Zhang, K., Chen, L., Li, Y., Brookes, P.C., Xu, J., Luo, Y. (2020) Interactive effects of soil pH and substrate quality on microbial utilization. European Journal of Soil Biology 96, 103151.

6 Acknowledgement

There comes a moment, once the long furrow is ploughed and the harvest almost gathered, when one turns to count every steadying hand along the way.

First, I express my sincere gratitude to Prof. Ingrid Kögel-Knabner, who unlocked the secret garden of soil science for me. She continuously challenged me to reflect deeply on the real-world significance behind every research question, sharpened my scientific reasoning and logic, and stood firmly behind my decisions. Her relentless curiosity and enthusiasm set a standard I aspire to throughout my scientific career.

Equally cherished is Dr. Franziska Bucka, who opened the doors of the BOKU family and greeted every fledgling notion with encouragement and kindness. Her positive feedback has greatly built my confidence and guided me through the challenges of navigating a new environment.

Special thanks go to the BLIK II project, funded by the Bayerisches Staatsministerium für Umwelt und Verbraucherschutz [TKP01KPB78573], Dr. Reinhard Zeitler, and my wonderful colleagues along the way: Sebastian, Rebecca, Sigrid, Anna, Yuan, and Ruben. I also extend my gratitude to Prof. Jörg Völkel and Dr. Michael Dannenmann for their ongoing support. Thanks to Franziska Steiner, Christopher Just and Jincheng Han for proofreading this work.

I am deeply indebted to Dr. Peter Schad, Prof. Jörg Prietzel, and Dr. Werner Häusler for their generous mentorship and the invaluable knowledge they shared. Heartfelt thanks to Dr. Carmen Hoeschen for her patience, kindness, and guidance throughout my learning process with NanoSIMS. Behind every experiment stand each technician whose assistance was indispensable: Bärbel Deischl, Sigrid Hiesch, Michaela Henn, Christine Pfab, Gabriele Albert, Petra Bucher, Maria Greiner, Monika Heilmeier, Ciaran Harrington, and Gertraud Harrington. Their patience, understanding, and technical support have been fundamental to my research. Equal thanks to Sonja Rottler, Yasemin Neubauer, and Florian Schmalzl for helping navigate administrative processes, and to Sijin Kim, whose meticulous work in the laboratory was invaluable.

My heartfelt appreciation goes to my BOKU friends and colleagues who made my days joyful and make my daily journey from Munich to Freising meaningful: Chris, Pedro, Yahan, Noelia, Franzi (B. B & A. S), Steffen, Julian, Chiara, Narda, Gabi, Kristina, Lucas, Rodrigo, Thiago, Luis, Lauren, Cristina, Tianyi, and Haotian. Those Maté breaks and Cachaça evenings are my unforgettable memories. I am also grateful to Chiara and Dr. Mauro for the opportunity to study in Italy, cherishing the warm-hearted Italians I met and, of course, the delightful Italian cuisine.

Special gratitude to Hao Ni for her encouragement and support. To my dear friends Dingli Wu and Jincheng Han, our mountain adventures, both digital and real, will forever be cherished. Dacheng Wei, my dear roommate, who introduced me to a vibrant Chinese community in Germany, enriching my life with friendships including Yuan Jin, Peter Wang, Jian Shi, and Yucheng Zhang. My sincere thanks also to friends from my studies in the Netherlands: Renhao Xu, Yahan Hu, and Anna Wu, whose friendships strengthened even amidst pandemic disruptions, and to the Wang family in Edinburgh for their warm hospitality.

Finally, I extend my deepest thanks to my parents (Weiyan Huang & Zhihong Lei) and families, whose unconditional support, trust, and love have profoundly shaped my journey. Their wisdom and guidance continually illuminate my path.

To everyone who walked beside me on this winding yet generous road: your fingerprints are on every page. This work is as much yours as it is mine.

Kaiyu Lei

Munich, May 2025

7 Appendix

A Study I

Kaiyu Lei*, Franziska B. Bucka, Christopher Just, Sigrid van Grinsven, Sebastian Floßmann, Michael Dannenmann, Jörg Völkel, Ingrid Kögel-Knabner

Distinct impact of land use and soil development processes on coupled biogeochemical cycling of C, N and P in a temperate hillslope-flood plain system

Biogeochemistry 168, 21 (2025). DOI: 10.1007/s10533-025-01213-y

B Study III

Kaiyu Lei*, Franziska B. Bucka, Pedro P. C. Teixeira, Franz Buegger, Christopher Just, Ingrid Kögel-Knabner

Balance organic and inorganic carbon in enhanced rock weathering: Implication for carbon sequestration

Global Change Biology 31, 4 (2025). DOI: 10.1111/gcb.70186

C Study II

Kaiyu Lei*, Franziska B. Bucka, Carmen Hoeschen, Yahan Hu, Ingrid Kögel-Knabner

Phyllosilicates determine the retention and availability of P in temperate soils

Unpublished

D Scientific contributions

Peer-reviewed publications

Lei, K., Bucka, F.B., Just, C., van Grinsven, S., Floßmann, S., Dannenmann, M., Völkel, J., Kögel-Knabner, I. (2025a) Distinct impact of land use and soil development processes on coupled biogeochemical cycling of C, N and P in a temperate hillslope-flood plain system. Biogeochemistry 168, 21.

Lei, K., Bucka, F.B., Teixeira, P.P., Buegger, F., Just, C., Kögel-Knabner, I. (2025b) Balancing Organic and Inorganic Carbon Dynamics in Enhanced Rock Weathering: Implications for Carbon Sequestration. Global change biology 31, e70186.

Conference contributions (first-authored)

Lei, K., Bucka, F. B., Teixeira, P. P., Buegger, F., & Koegel-Knabner, I. (2025). The enhanced rock weathering stages determine the fluxes and interactions of soil inorganic and organic carbon pools (No. EGU25-8352). Copernicus Meetings.

Lei, K., Bucka, F. B., Höschen, C., Hu, Y., and Kögel-Knabner, I.: Exploring spatial distribution and characterization of inorganic and organic phosphorus in temperate soils using NanoSIMS, EGU Gen eral 2024, Vienna, Austria,14-19 Apr 2024, EGU24 21972.

Lei, K., Bucka, F., van Grinsven, S., Völkel, J., and Kögel-Knabner, I.: Changes in soil carbon, nitro gen, phosphorus along two temperate slope-floodplain-creek catenas under different land use - A case study in Southeast Germany, EGU General Assembly 2023, Vienna, Austria, 24-28 Apr 2023, EGU23 1544.